Forensic Sci Med Pathol (2016) 12:451–485
DOI 10.1007/s12024-016-9776-y

ORIGINAL ARTICLE

Methods for determining time of death

Burkhard Madea[1]

Accepted: 18 March 2016 / Published online: 4 June 2016

Abstract Medicolegal death time estimation must estimate the time since death reliably. Reliability can only be provided empirically by statistical analysis of errors in field studies. Determining the time since death requires the calculation of measurable data along a time-dependent curve back to the starting point. Various methods are used to estimate the time since death. The current gold standard for death time estimation is a previously established nomogram method based on the two-exponential model of body cooling. Great experimental and practical achievements have been realized using this nomogram method. To reduce the margin of error of the nomogram method, a compound method was developed based on electrical and mechanical excitability of skeletal muscle, pharmacological excitability of the iris, rigor mortis, and postmortem lividity. Further increasing the accuracy of death time estimation involves the development of conditional probability distributions for death time estimation based on the compound method. Although many studies have evaluated chemical methods of death time estimation, such methods play a marginal role in daily forensic practice. However, increased precision of death time estimation has recently been achieved by considering various influencing factors (i.e., preexisting diseases, duration of terminal episode, and ambient temperature). Putrefactive changes may be used for death time estimation in water-immersed bodies. Furthermore, recently developed technologies, such as H magnetic resonance spectroscopy, can be used to quantitatively study decompositional changes. This review addresses the gold standard method of death time estimation in forensic practice and promising technological and scientific developments in the field.

Keywords Time of death · Methods · Body cooling · Nomogram method · Vitreous humor · Decomposition

Introduction

Estimating the time of death is an important task in daily forensic casework. Research addressing the time of death should always be performed with this in mind. However, many papers on this subject describe only the time dependence of a postmortem analyte or parameter that has no value in forensic practice.

The main principle behind determining the time of death is calculation of data that can be measured back to the starting point along a time-dependent curve. The characteristics of the curve (e.g., the slope) and the starting point (the time of death) are influenced by internal, external, antemortem, and postmortem conditions (Fig. 1). Because the starting point and the slope of the curve are influenced by multiple factors (e.g., ambient temperature or local temperature at the measurement site), the estimated time of death is calculated as a period of time rather than a single point in time [1–6].

Various parameters are currently used to estimate the time of death (Table 1), including:

- Body cooling [7–26], postmortem lividity [27–30], and radiocarbon dating [31], which are predominantly physical processes;

✉ Burkhard Madea
b.madea@uni-bonn.de

[1] Institute of Forensic Medicine, University of Bonn, Stiftsplatz 12, 53111 Bonn, Germany

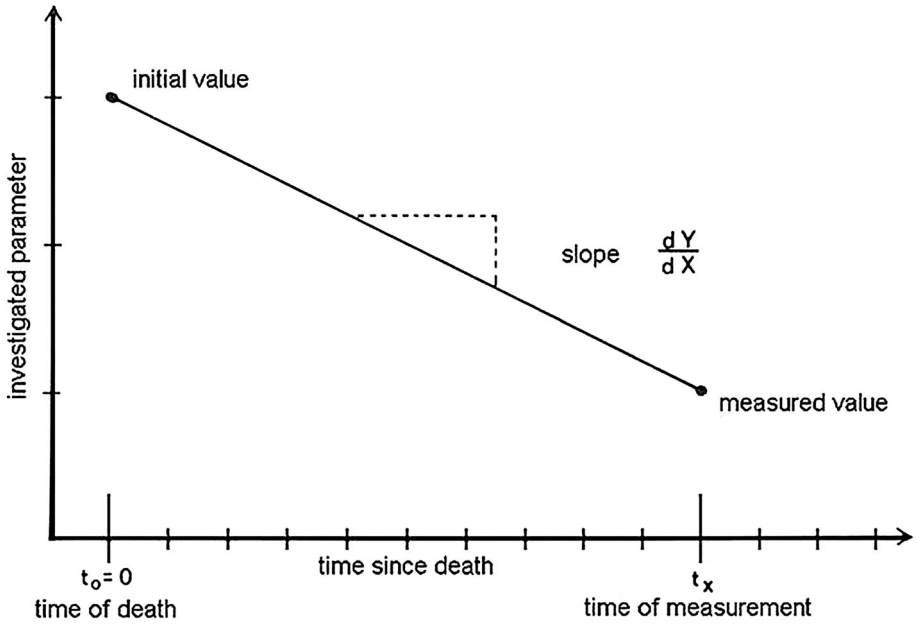

Fig. 1 Main principle of determination of time since death (calculation from a measured value along a curve back to the initial value)

Table 1 Postmortem changes used to estimate time since death

Purely physical processes	Body cooling, hypostasis
Metabolic processes	Supravital reactions
Autolysis	Loss of membrane permeability, diffusion
Physicochemical processes	Rigor mortis
Bacterial processes	Putrefaction

- Rigor mortis [32–43] and supravital reagibility of skeletal muscle [44–50], which are physicochemical processes;
- Putrefaction [51–56], which is mainly based on bacterial processes;
- Chemical methods, which are based on metabolic processes, autolysis, and diffusion according to the concentration gradient [57–88]; and
- Entomology [89–92].

These methods for estimating the time of death are not only different in nature but also in their scientific value, their underlying scientific processes, and their methods of data validation [4–6] (Table 2).

Some methods of estimating the time since death take into account influencing factors such as ambient temperature and rely on extensive quantitative measurements with mathematical descriptions of time changes. Clear data are available on the precision of these methods for estimating time since death, with precision being determined using independent case material (e.g., body cooling). Some alternative methods are based on a subjective grading of postmortem change, while other methods are based solely on empirical data (i.e., empirical knowledge; no controlled longitudinal or cross-sectional studies) and not on statistically evaluated reference values.

Caseworkers must keep in mind the range of validity among the various methods of estimating the time of death with respect to the experimental background, study type, influencing factors, and statistical evaluation. Of highest evidential value are methods incorporating the following:

- longitudinal studies on well-characterized reference samples;
- mathematical descriptions of postmortem changes;
- clear data on the precision of the estimated time of death;
- high precision of the estimated time of death as proven by independent control samples; and/or
- field studies on the applicability of the method in practice.

These methods should replace other less reliable methods of estimating the time of death. Early forensic pathologists were aware of the problems in death time estimation. For instance, Van den Oever [93] wrote in a review: “for about 30 years forensic scientists have tried hard to solve this problem by developing a method that would permit the determination of the exact time of death, but the results of all these often very extensive studies show clearly that the moment of death can only be fixed within certain limits of probability.”

Table 2 Grading of methods of estimating time since death regarding mode of registration of postmortem change; description, influencing factors; and calculation of confidence limits

1. Quantitative measurement: mathematical description, quantitatively taking influencing factors into account, declaration of precision, proof of precision on independent material, field studies
Examples: body cooling (nomogram method); potassium concentration in vitreous humor
2. Subjective description (grading): consideration of influencing factors, declaration of precision, proof of precision on independent material
Example: supravital reactions
3. Subjective description of postmortem changes: influencing factors known "in principle," empirical estimations instead of statistically evaluated reference values
Examples: rigor mortis, lividity
4. Subjective description: analogous conclusions based on empiricism and assumptions instead of statistically evaluated reference values
Example: gastric contents
5. Subjective description: velocity of progression of postmortem changes entirely depending on ambient factors; no sound empirical estimation possible because of the broad spectrum of ambient factors
Example: putrefaction

Camps [94] concluded: "further, it must have a true scientific backing both on an experimental and statistical basis for otherwise the evidence might possibly be dangerous to the interests of justice…I would suggest that our aim should be to obtain a figure with as small a margin of error as possible; in fact, I would say that it is better to prove without contradiction that death *could* have occurred at a time when a certain person was there, rather than it *did* occur at some exact moment."

Objectives of time of death estimation

There are two approaches to estimating the time of death [1]: (1) evaluation of antemortem changes, either physiological or pathological, which can be detected in the body and combined with conclusions from investigations by the police (survival time); and (2) evaluation of postmortem changes, which allows the investigator to draw a conclusion about the time of death. The first approach comprises methods such as wound age estimation or evaluations based on gastric contents [95–100], which usually yield only rough estimations of the time of death.

The second approach is more important. It comprises the spectrum of methods based on progressive postmortem changes, which are usually evaluated at the crime scene. If the time of death and time of assault are not identical, however, it is necessary to combine the two approaches to gain an impression of how long the patient lived after the injury and when death occurred after the assault.

Police further use non-scientific criminalistic or scene markers, such as the dates on the most recent mail or newspapers received by the individual or when the individual was last seen alive by neighbors [79, 101]. Medical estimation of the time of death at a crime scene is used for different purposes [1, 101]. For example, it may be used to give the police a preliminary idea of the time of an assault (although it should be noted that the time of death gives information on the time of assault only in cases with a short survival period. The actual time must be established based on autopsy findings); or to determine whether the time of death is consistent with the alibi of a suspect. Only in rare cases does the time of death play a major role in court proceedings as the only evidence regarding the guilt of a suspect. Precision is important in estimations of time of death, but the reliability is even more important. A highly precise but unreliable result may cause police investigations to be misled for a considerable time.

We offer here only a brief review on the methods used to estimate the time of death; detailed explanations of individual methods can be found in the literature [1, 4–6, 21, 101]. In addition, several relevant historical reviews have been published on the subject [60, 93, 94, 97, 102].

Death and dying

Death and dying are processes characterized by loss of function and coordination of the major organ systems (cardiovascular, respiratory, and nervous systems). Loss of coordination among these systems involves dissociation of the organs' functions. The agonal period may be initiated by disease or trauma. The final crisis results in vita minima (state of apparent death), during which no vital signs are apparent. Ultimately, the death of the individual is characterized by irreversible cessation of circulation or respiratory arrest (Fig. 2). Under special clinical conditions, brain death may replace the classic signs of death (irreversible circulatory or respiratory arrest and their consequences, i.e., postmortem lividity and rigor mortis). The

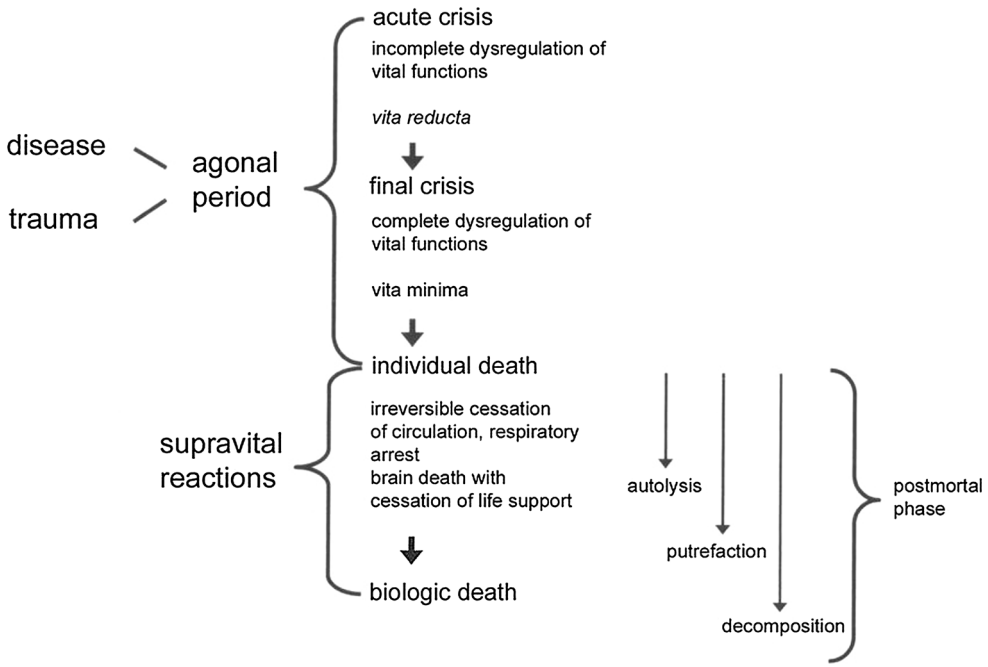

Fig. 2 Scheme and terms of the agonal period. The agonal period is initiated either by disease or trauma

duration of the agonal period may vary greatly. Ultra-rapid agonal periods may be found after an explosion, with total dismemberment of the body in milliseconds; short agonal periods of some minutes' duration are found with many violent deaths and acute natural deaths; and long-term episodes lasting hours to days are seen in terminal episodes of long-lasting diseases (e.g., cancer). The duration of the agonal period may be an important factor in the progression of postmortem changes [4, 6].

Supravitality

Irreversible circulatory or respiratory arrest is, in most cases, the main criterion for death. Tissue metabolism, however, does not cease immediately after death but continues for some hours [50, 103]. During the early postmortem period, the main energy-producing metabolic processes are the creatine kinase reaction and anaerobic glycolysis. During this period of intermediary life, supravital reactions—defined as postmortem excitation-induced reactions of tissues—can be examined. The duration of the supravital period is much longer than that of the resuscitation period, a fact established based on physiology and experimental surgery (Fig. 3). The resuscitation period is the time of global ischemia, after which the ability to recover expires. The supravital period that follows is characterized by increasing irreversible structural and functional damage. The resuscitation period for skeletal muscle under normothermia lasts approximately 2–3 hours postmortem (hpm), and supravital electrical excitability of skeletal muscle may be preserved for up to 20 hpm. Some supravital reactions are of great practical importance in forensic medicine because they can be easily examined at the crime scene and provide an immediate result regarding the time elapsed since death. These reactions include mechanical and electrical excitability of skeletal muscle and pharmacologically induced excitability of the iris.

Mechanical excitability of muscle

The mechanical excitability of skeletal muscle is examined by rigorously hitting a muscle with the back of a knife or chisel (e.g., the biceps brachii muscle is hit at right angles to the arm axis). Other muscles can also be examined, but reference values for estimating the time of death are available only for the biceps brachii muscle [43, 44, 50]. The muscle exhibits one of the following three reaction patterns depending on the postmortem interval (PMI) (Fig. 4). During the first phase of mechanical excitation, the whole muscle contracts (propagated excitation). This idiomuscular contraction is identical to Zsako's muscle phenomenon. The first degree of idiomuscular contraction, propagated excitation, can be observed for as long as 1.5–2.5 hpm. During the second phase, a strong, typically reversible idiomuscular pad develops. This phase may be seen as for long as 4–5 hpm (Fig. 5). During the last phase, a weak idiomuscular pad develops and may persist over a longer period (up to 24 h). This can be observed for as long as 8–12 hpm. If the idiomuscular pad is not visible, it should be sought by palpation. Otherwise, a skin incision may be necessary to demonstrate its presence.

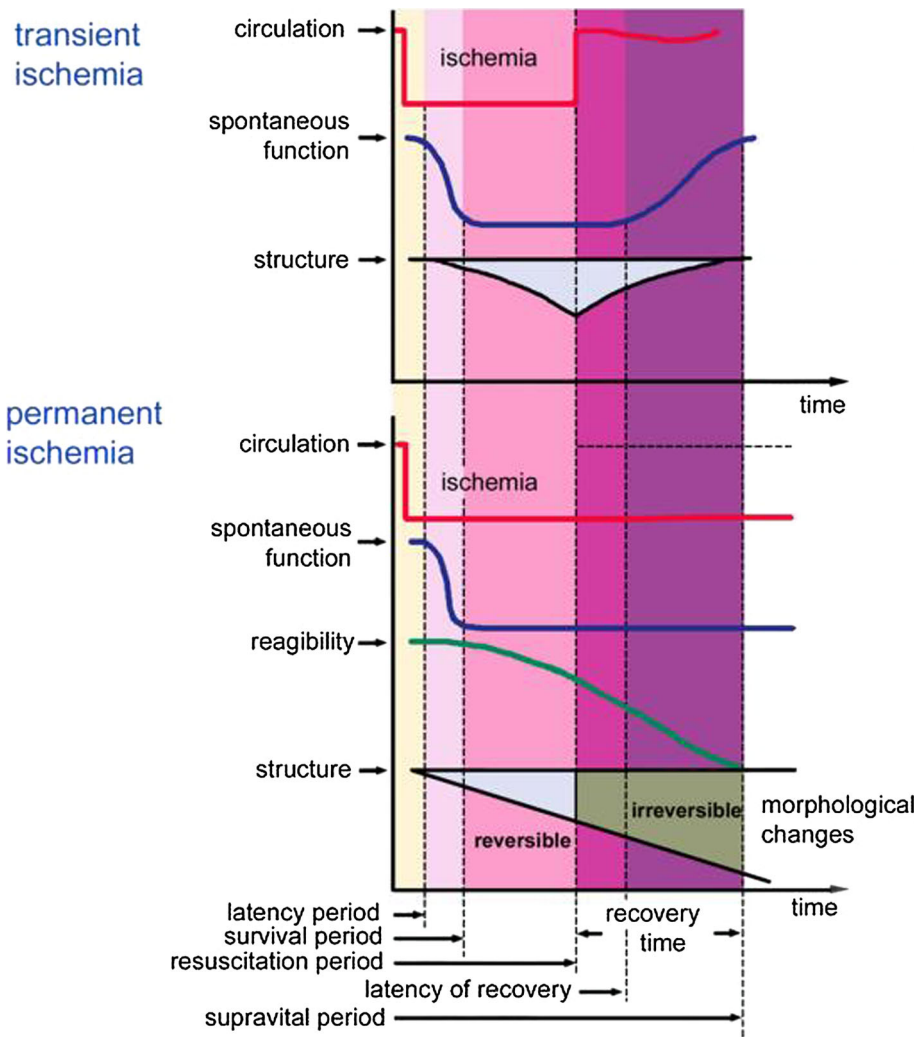

Fig. 3 Diagram of duration of supravital period (*bottom*) compared with resuscitation period (*top*). The supravital period after irreversible circulatory arrest greatly exceeds the duration of the resuscitation period after transient ischemia

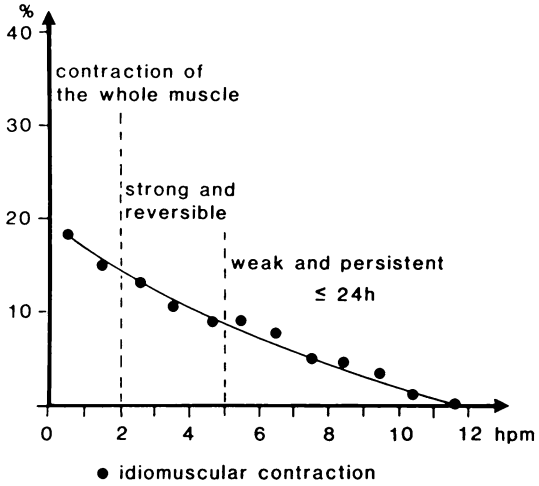

Fig. 4 Three phases of idiomuscular contraction after mechanical excitation of the muscle; frequency of a positive reaction (*y*-axis) over the postmortem interval (*x*-axis)

Electrical excitability of skeletal muscle

The first investigations on electrical excitability of skeletal muscle were carried out at the end of the 18th century and beginning of the 19th century. The results of these studies indicated that the electrical excitability of skeletal muscle could be recommended as a method for estimating the time of death [97, 102]. Extensive investigations have also been carried out to objectively assess muscular contraction [45–47, 49]. For practical purposes, most investigations on postmortem electrical excitability of skeletal muscle are based on a verbal description and subjective grading of the muscular response to excitation (i.e., the muscular contraction) according to the strength of the contraction and the spread of movement to areas distant from the electrodes [48–65].

Early PMI excitation leads to strong contraction of muscles. The excitation then spreads to muscles distant

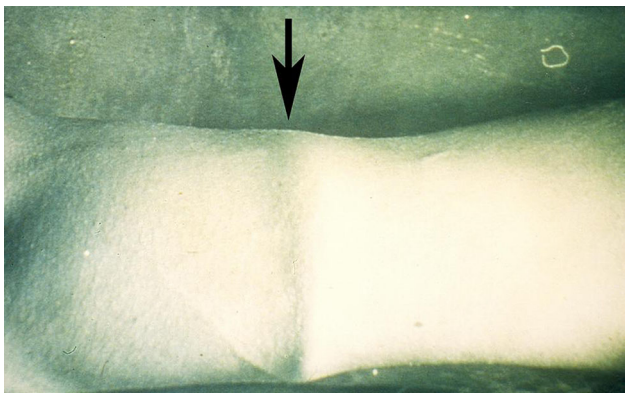

Fig. 5 Typical idiomuscular pad of the biceps brachii muscle

from the electrodes. The contraction weakens with an increasing PMI, and the muscular response is confined to the site of excitation. This reaction pattern can be seen to some extent in all muscles. Finally, only fascicular twitching or movement of the electrodes is visible. The most extensive investigations have been carried out for the orbicularis oculi muscle because movements of this muscle are easily visible. For this measurement, puncture electrodes are inserted 5–7 mm deep into the nasal part of the upper eyelid and 15–20 mm apart from one another (Fig. 6). The muscular response is graded into 6° intervals. During the very early PMI (degree VI), the entire ipsilateral muscle contracts. In degree V, only the upper and lower eyelids and forehead muscles contract. With increasing postmortem duration, the reaction becomes confined to the site of excitation (Fig. 7; Table 3).

A small square wave generator producing constant-current rectangular impulses of 30 mA (10-ms duration, 50-ms repetition rate) was used for stimulation (Fig. 8). The mean grading values and 95 % confidence intervals (CIs) for the degrees are presented in Fig. 7.

The 95 % CIs for 6° of electrical excitability of the orbicularis oculi muscle have been proven reliable using independent case material and in field studies. However, in the presence of hematoma or emphysema of the eyelid, electrical excitability may last much longer than that corresponding to the upper 95 % CI for the particular degree (Table 3, last column). The same is true in cases of hypothermia. In contrast, the duration of electrical excitability is shorter in cases involving chronic diseases with a long terminal period than in cases of sudden death because glycogen, which is responsible for re-synthesis of adenosine triphosphate, may have been depleted during life.

Other muscles can also be examined. Reliable reference data are available for various muscles, including the orbicularis oris muscle (Fig. 9). Additionally, the muscles of the thenar and hypothenar eminences may react to stimulation for as long as about 11 hpm.

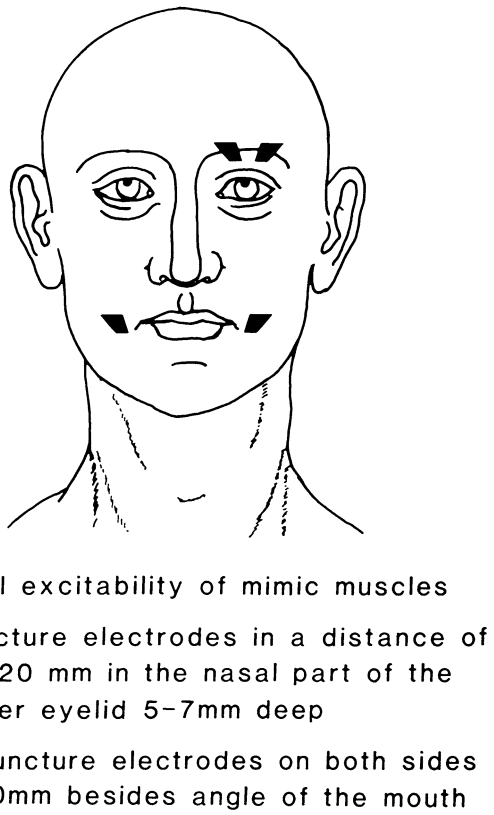

Fig. 6 Position of electrodes for examining electrical excitability of facial muscles

Pharmacologically induced excitability of the iris

Compared with skeletal muscle, the smooth iris muscle is irritable in response to electric and pharmacologic stimulation for quite a long period. In some cases, excitability created by subconjunctival injection of norepinephrine or acetylcholine may be preserved up to 46 hpm (Table 4). For practical purposes, pharmacologic excitation of the iris after subconjunctival injection of drugs is recommended. The drugs should not be injected into the anterior chamber [65]. The diameter of the pupil should be recorded before injection using a transparent, multidiameter pattern. About 0.5 ml of norepinephrine, tropicamide, atropine, or acetylcholine solution should be injected. A positive reaction is seen within 5–30 min and may be characterized by either an increased diameter (e.g., atropine, tropicamide, and norepinephrine) or a decreased diameter (e.g., acetylcholine). The reaction lasts at least 1 h. When no change is visible after this time, the reaction is considered negative (Table 4). It is sufficient to examine the pharmacologic excitability of the iris with only one drug because examining a double reaction after injecting a mydriatricum followed by a mioticum does not give further information about the time of death.

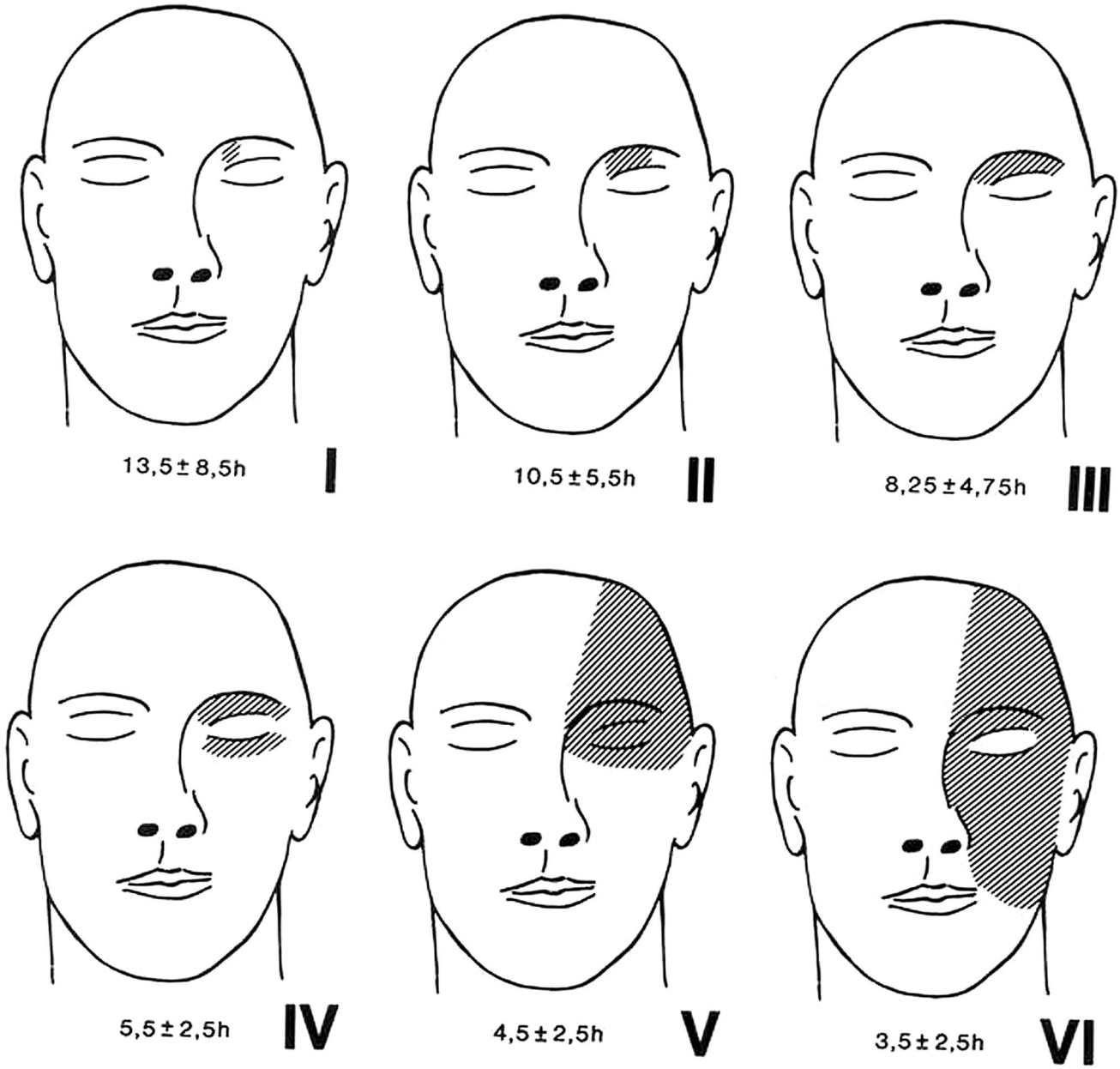

Fig. 7 Six degrees of positive reaction after stimulation of the orbicularis oculi muscle (see Table 3 also)

Other supravital reactions include the response of sweat glands upon injection of drugs, sperm motility, leukocyte vitality, DNA incorporation, and postmortem blood clotting. These supravital reactions, however, have no practical relevance in forensic medicine.

Postmortem lividity

After irreversible circulatory arrest, lividity develops as the earliest postmortem change. After circulatory arrest, the hydrostatic pressure becomes the leading force within the parallelogram of forces comprising blood pressure, structural barriers, tissue turgor, and the pressure of underlying surfaces [1, 4, 6, 28]. Hypostasis is defined as the movement of body fluids under the influence of gravity. All fluid compartments are involved in hypostasis, including intravascular and transcellular fluids. Influenced by gravity, blood moves into the lowest parts of the vascular system; in the supine position, it flows into the back, buttocks, thighs, calves, and back of the neck. Irregular pink patches in the face, especially the cheeks, during the agonal period are caused by local stasis and are called *Kirchhofrosen* (Table 5). Postmortem lividity visible in the skin is a

Table 3 Upper and lower confidence limits for the six degrees of electrical excitability in hours in different random samples

Degree		Forensic pathology	Clinical pathology	Hematoma/emphysema of the eyelid
I	Local upper eyelid	5–22	3–16	29 traumatic emphysema 27.3–52 postmortem emphysema 32 traumatic hematoma
II	One- to two-thirds of upper eyelid	5–16	0–16	
III	Whole upper eyelid	3.5–13	1.5–9	
IV	Upper and lower eyelid	3–8	1–7	
V	Upper and lower eyelid + forehead	2–7	1–7	
VI	Upper and lower eyelid + forehead + cheek	1–6	1–6	

Forensic pathology: shorter terminal episode

Clinical pathology: longer terminal episode (shorter duration of electrical excitability than in cases of forensic pathology)

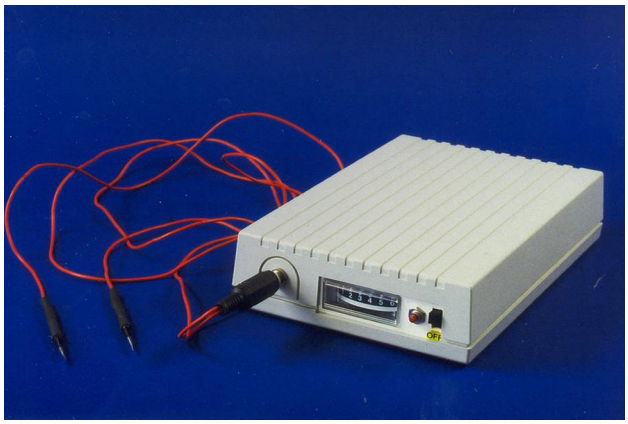

Fig. 8 Square wave generator for defined muscle stimulation (e.g., facial muscles), enabling procurement of the data in Table 3 and Fig. 7. Producer and supplier: Peschke J, http://home.t-online.de/home/j-peschke/rztg1.htm

consequence of the movement of blood into the capillaries of the corium. Postmortem lividity may be visible 20–30 min postmortem, appearing during the early stages as still pink patches that gradually coalesce with the increasing PMI. Because of consumption of oxygen, the pink color changes to dark pink or blue.

Of predominant criminalistic significance is the phenomenon of disappearance of lividity on pressure and after turning the body. During the early stages, lividity completely disappears upon soft thumb pressure. With increasing PMI, the pressure required to cause disappearance of lividity must increase as well. Later, lividity disappears only incompletely with pressure and eventually does not disappear at all.

If the body is turned during an early PMI, some or all of the hypostasis may move downward to new areas. In a comparatively later PMI, only some of the hypostasis moves down into the new area, and only slight blanching is noted in the original area (Fig. 10).

With increasing PMI, the disappearance of lividity on thumb pressure and its relocation after shifting decreases before ceasing completely. This is caused by an increasing hemoconcentration of intravascular erythrocytes due to transcapillary plasma extravasation (i.e., the fluid moves from the blood, leaving behind the red blood cells, which cannot move without the liquid). Intravascular hemoconcentration is the main reason for the gradually decreasing disappearance of lividity upon thumb pressure and after shifting. In a comparatively later PMI, there is hemolysis with hemoglobin diffusion into the perivasal tissue. This phase, however, is only a secondary mechanism contributing to the fixation of hypostasis.

The stepwise phases of hypostasis are: beginning, confluence, maximum, disappearance on thumb pressure, complete or incomplete disappearance after shifting, and changing with time. No longitudinal studies on these phases have been performed using large random samples, and extant studies are of limited value. The best statistical data available were summarized by Mallach [29] and Mallach and Mittmeyer [30], who calculated mean values, standard deviations, and 95 % CIs based on textbook reports (Table 6). These data remain undisputed because better data are unavailable. It should be noted, however, that they do not represent absolute values. Investigations with a quantitative measurement of livor mortis are not currently considered of practical importance.

Definitions of these hypostasis phases are as follows.

- In the *beginning* mottled patches appear on the lower parts of the body (e.g., the back of the neck in the supine position).
- *Confluence* is identified by the presence of separate areas of discoloration of moderate intensity.

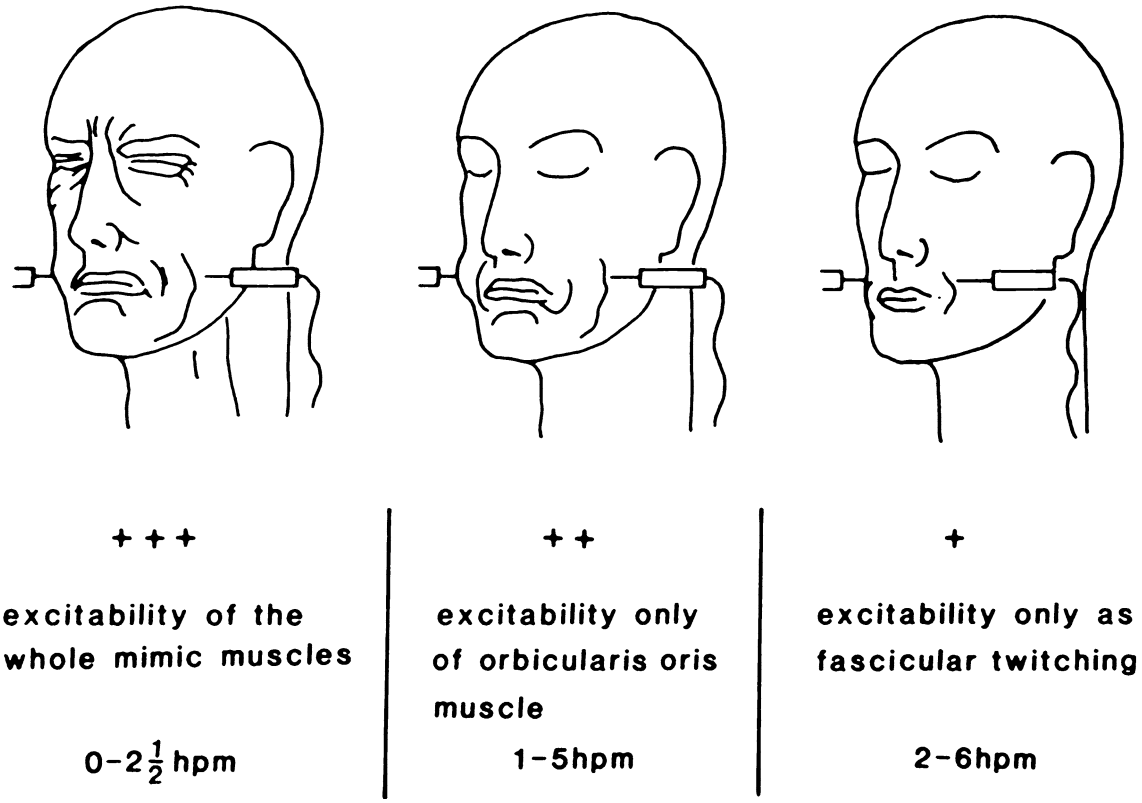

Fig. 9 Three degrees of positive reaction after stimulation of the orbicularis oris muscle

Table 4 Postmortem excitability of the iris after injection of different drugs

Drug	%	Postmortem excitability (h)
Mydriatics		
Norepinephrine/epinephrine	1	14–46
Tropicamide	0.25	5–30
Atropine/cyclopentolate	1/0.5	3–10
Miotics		
Acetylcholine	5	14–46

- *Maximum* hypostasis is identified if hypostasis does not increase during the crime scene investigation or at autopsy.
- *Thumb pressure* is considered positive if lividity disappears completely on light thumb pressure.
- *Complete relocation* is when all hypostasis shifts downward to the new dependent areas (e.g., when a body is turned from a face-down to a supine position at the scene).
- *Incomplete shifting* is identified when hypostasis remains in the former dependent areas but also shifts to new dependent areas.

Rigor mortis

After primary flaccidity, the second postmortem change and sign of death is rigor mortis, which develops in normal ambient temperature at about 3–4 hpm. Rigor mortis was misjudged as a sign of death up to the 19th century, although Shakespeare (*Romeo and Juliet*, Act 4, Scene 1) described all elements of rigor mortis very well: "Each part, deprived of supple government, shall, stiff and stark and cold, appear like death."

With irreversible circulatory arrest, all muscles of the body become completely flaccid due to loss of tone. During the early PMI, adenosine triphosphate, the chemical source of energy, can be resynthesized via the creatine kinase reaction and anaerobic glycolysis [32, 33]. Once the adenosine triphosphate level has fallen to <85 % of the initial value, actin and myosin filaments contract and the subjective impression of stiffening of the muscle sets in (Table 7). In practice, the development and state of rigor mortis are proved subjectively by flexing a joint; either the muscles are flaccid or, during development of rigor mortis, resistance may be felt (Fig. 11). If rigor has fully developed, even a strong investigator cannot flex or stretch the joint. The biochemical, physiologic, and mechanical

properties of rigor (including before and after rigor) are summarized in Table 7.

Rigor must not be mistaken for cold stiffening. When rigor is present, hypostasis must be present as well. Hypostasis is absent in cases of cold stiffening (body core temperature of 30–33 °C).

The development and state of rigor should be examined in several joints (e.g., the mandibular, finger, knee, and elbow joints) to determine if it is still progressing or has already reached its maximum.

Rigor mortis does not start in all muscles simultaneously. Nysten's rule (1881), that rigor starts in the mandibular joint and then progresses to the muscles of the trunk, lower extremities, and upper extremities, is usually true when death occurs in the supine position. However, rigor starts in the lower extremities when glycogen depletion occurs in the lower extremities during agony [97].

Resolution of rigor mortis is due to protein degradation with increased ammonia (NH_3). Rigor does not start simultaneously in muscle fibers, but progresses successively. This phenomenon can be used to establish a rough estimate of the time of death. If some fibers have already become stiff, the stiffness can still be broken by flexing a joint; rigor then develops in other fibers that have not yet stiffened. Depending on the time point at which the stiffness is broken, rigor may develop again at a higher or lower level unless it was already fully developed (Fig. 12). This phenomenon of reestablishment of rigor mortis may be seen for as long as 6–8 hpm or, at very low ambient temperatures, for up to 12 hpm. More recent investigations have claimed reestablishment of rigor mortis at a much longer PMI, but the evidence they offer is not convincing, and the investigations are not reliable [42].

Secondary flaccidity may become apparent at normal ambient temperature after 2 days. At low ambient temperatures, fully developed rigor mortis may be preserved for $\geq$2 weeks. Cadaveric rigidity, cataleptic spasm, and instantaneous rigor are phenomena mentioned in textbooks but nonexistent in practice. No reported cases involving these phenomena have stood up to criticism.

Rigor mortis is established in both skeletal and smooth muscle (e.g., in skin). Rigidity of the smooth arrector pili muscles appears as gooseflesh (cutis anserina).

Development, duration, and resolution of rigor mortis depend on several factors, including the amount of glycogen in the muscle at the moment of death and the ambient temperature. Therefore, rigor may develop rapidly in persons who die during or soon after physical exertion or exhaustion, or from electrocution. All of the above-mentioned phases of rigor mortis (development, reestablishment, full development, duration, and resolution) are time-dependent. This became evident in one of the rare studies of rigor mortis in the 19th century. Niderkorn, who determined the times necessary for completion of rigor mortis in

Table 5 Lividity: causes, consequences, and phenomena checked on the body

Lividity: causes, consequences and phenomena checked on the body				
Cause		Consequences		Phenomenon
Decrease of force of myocardial contraction	→	Stasis	→	"Kirchhofrosen", local stasis with patchy discoloration during agonal period due to centralization of circulation
Cardiac arrest, hydrostatic pressure	→	Hypostasis	→	Livores with a "shifting" quality and "disappearance on pressure"
Vascular permeability	→	Hemoconcentration	→ ↘	Decrease of shifting and disappearance on pressure
Autolysis, putrefaction	→	Diffusion of haemoglobin	→	No shifting, no disappearance on pressure

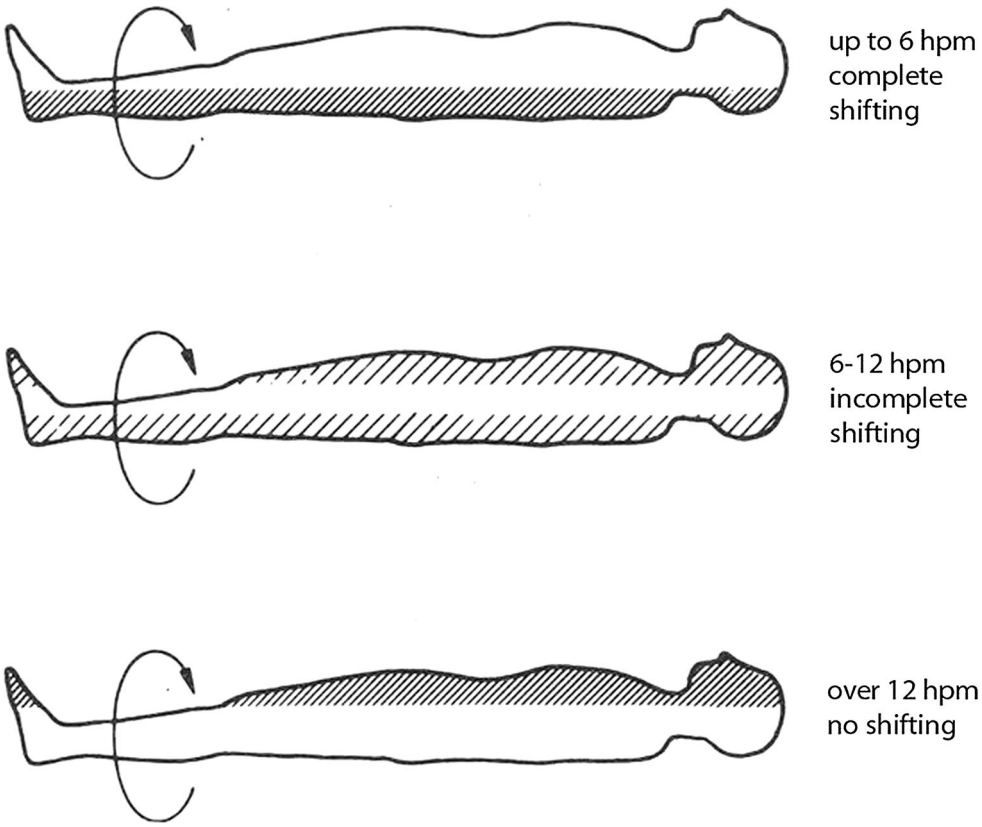

Fig. 10 Shifting of lividity after turning the body

Table 6 Time course of different criteria of lividity

	$\bar{x}$	s	2 s		Range of scatter		Number of quotations
			Lower limit	Upper limit	Lower limit	Upper limit	
Development	¾	½	–	2	¼	3	17
Confluence	2½	1	¾	4¼	1	4	5
Greatest distension and intensity	9½	4 ½	½	18¼	3	16	7
Displacement							
1. Complete on thumb pressure	5½	6	–	17½	1	20	5
2. Incomplete on sharp pressure (forceps)	17	10 ½	–	37½	10	36	4
Displacement after turning the body							
1. Complete	3¾	1	2	5½	2	6	11
2. Incomplete	11	4½	2¼	20	4	24	11
3. Only slight pallor	18½	8	2½	34½	10	30	7

Statistical calculations performed by Mallach [29] on textbook reports. The statistical calculations are not based on cross-sectional or longitudinal studies but on empirical knowledge quoted in textbooks. $\bar{x}$ = mean value; s = standard deviation

113 bodies, found that it was fully established after 4–7 hpm in 76 bodies (67 %) and that rigidity was complete within 2 hpm in 2 bodies and within 13 hpm in 2 bodies [2, 97].

Great inter-individual variability exists owing to endogenous and exogenous factors. Longitudinal studies on large random samples are lacking, although animal experiments taking into account various factors influencing the time course of rigor mortis have been performed. Devices for objective measurement of rigor mortis have been developed but are not yet practically important.

The best available data, despite all justified criticism, are from Mallach [29] and Mallach and Mittmeyer [30], based on a literature compilation of reports spanning 1811–1969, with statistical analysis (Table 8). However, these values cannot be claimed to be absolute. As for lividity, rigor

Table 7 Overview of biochemical, mechanical, morphological, and physiological bases of rigor mortis

	Delay period	Establishment of rigor	Rigor phase	Postrigor phase, secondary flaccidity
Biochemistry	ATP level: 0.435 ± 0.555 mg/g muscle	ATP level decreased to <85 % of the original value	–	NH_3↑
Mechanics	–	Stiffness ↑, plasticity first increased, then decreased. Contraction of loaded muscle	–	Spontaneous elongation of loaded muscle; plasticity ↑
Morphology	–	Appearance of fine transverse striations (bridging between A and I filaments) with a periodicity of 400 Å	Swelling and destruction of mitochondria and sarcoplasmic reticulum	Irreversible elongation of muscle; decoupling of myofilaments, disintegration of structure
Physiology	Exponential decrease in membrane potential: above −55 mV, propagated excitation possible; below this level and up to −30 mV, only local concentration on excitation	–	–	–

ATP adenosine triphosphate

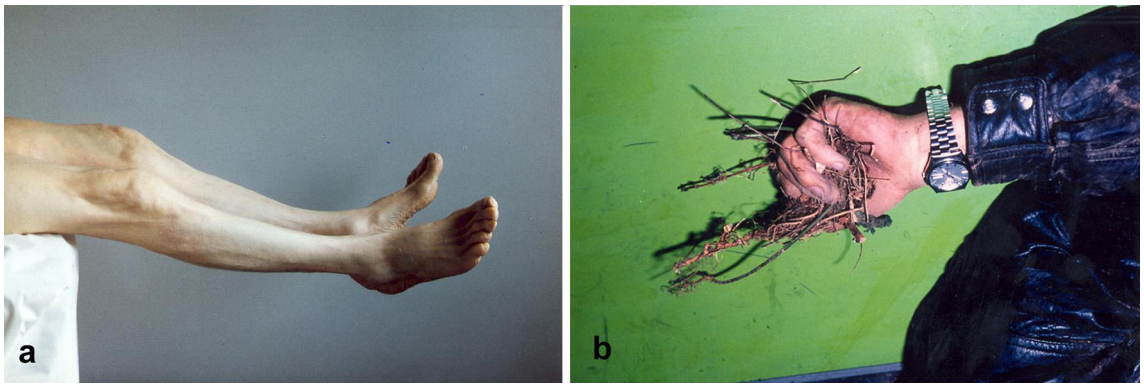

Fig. 11 The lower leg is fixed against gravity because of rigor mortis (Fig. 12A). Objects like branches in the hand must not be mistaken for instantaneous rigor mortis or cadaveric spasm

Table 8 Time course of different criteria of rigor mortis

Rigor state	Average hpm and standard deviation	Rage of scatter in hours (2 s)		Number of quotations
		Lower limit	Upper limit	
Beginning	3 ± 2	–	7	26
Maximum	8 ± 1	6	10	28
Duration	57 ± 14	29	85	27
Complete resolution	76 ± 32	12	140	27

Data are according to calculations by Mallach [29] based on textbook reports

hpm hours postmortem

mortis provides only a rough estimation, and no accuracy can be expected. Rigor mortis should, thus, never be the only criterion used.

In summary, rigor is examined by flexing or stretching the joints. Its beginning is established when slight rigor is observed in some joints. Complete or maximum development of rigor means that it has strongly developed in all joints. Reestablishment is present when rigor is found again in a joint (mostly the elbow) some hours after breaking the rigor. Rigor is usually broken during the crime scene investigation and evaluated again at autopsy.

Algor mortis

The postmortem decrease in body temperature is the result of four activities: convection, conduction, radiation, and evaporation. Convection and conduction are the most important factors among the four. The rate of cooling depends on various conditions: ambient conditions (e.g., temperature, wind, rain, and humidity); the weight of the body and mass/surface area ratio; the posture of the body (extended or thighs flexed on the abdomen); and the clothing/covering.

Various temperature probe sites, such as the surface skin, axilla, liver, rectum, and brain, are used to determine the body temperature [2, 3, 9, 10, 104]. For practical purposes, only central core temperatures (e.g., rectum, brain) are of value today [13–16]. Body cooling does not follow Newton's law of cooling. As early as the nineteenth century, investigators using rectal temperature described a lag time—the postmortem temperature plateau—before exponential body cooling according to Newton's law [102] (Fig. 13). The temperature plateaus because central axial temperatures cannot begin to decrease until a heat gradient is established between the core and surface of the body. This delay is variable and may last several hours [22].

A mathematical expression of rectal cooling after death was published by Marshall and Hoare [26], who took into account the whole sigmoidal shape of the cooling curve [9, 22, 26]. They performed body-cooling experiments under "standard conditions of cooling," which they defined as a "naked body with dry surfaces, lying extended on a thermically indifferent base, in still air." Their mathematical model of body cooling was expressed in a two-exponential term:

$$Q = \frac{T_r - T_a}{T_0 - T_a},$$

$$A \times \exp(B \times t) + (1 - A) \times \exp \times t,$$

where Q = standardized temperature, T_r = rectal temperature at any time t, T_0 = rectal temperature at death ($t = 0$), T_a = ambient temperature, A = constant, B = constant, and t = time of death. The second exponential term is subtracted from Newton's exponential term, taking into account that while at first there is no temperature decrease, the temperature falls after the plateau phase. This mathematical expression is valid for all central axial temperatures and represents the ultimate success in modeling body cooling for the purpose of estimating the time of death. The exponential form with the constant B expresses the exponential drop in temperature after the plateau according to Newton's law of cooling. The term with the constant A as part of the exponent describes the postmortem temperature plateau. The experimental work that led to identification of these constants is outlined in several original papers and two monographs [1–3, 11–14, 22].

The nomogram method developed by Henssge [13, 14, 22] is the gold standard for determining the time of death. Empirically, it was found that the individual value of B could be computed under chosen standard conditions of cooling using the following equation:

$$B = -1.2815\left(\mathrm{bw}^{-0.625}\right) + 0.0284,$$

where bw = body weight (kg). This equation reflects the idea that body cooling after the temperature plateau is mainly influenced by body weight. Values for the constant

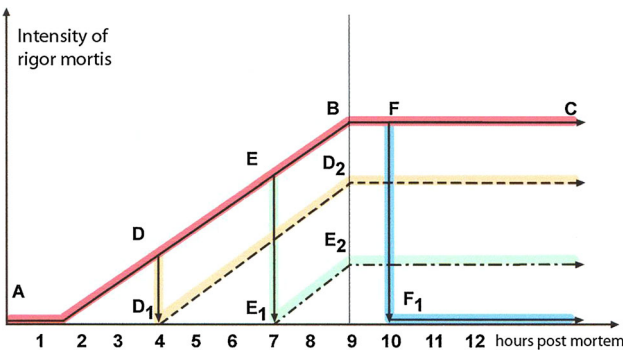

Fig. 12 Re-establishment of rigor mortis after breaking. The later rigor is broken during its development, the lower will be its level after re-establishment. If rigor is broken after it has already been fully developed (F), it will not be re-established at all

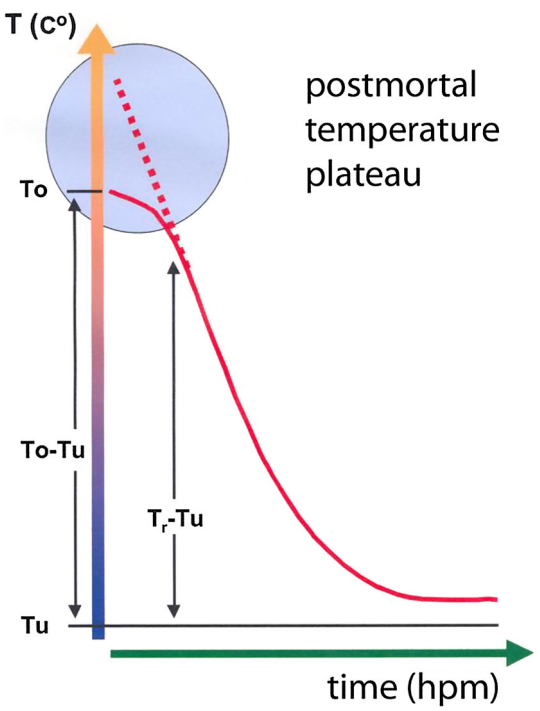

Fig. 13 Sigmoidal shape of the cooling curve, which is best described by Marshall and Hoares (two-exponential term). The quotient $\left(Q = \frac{T_r - T_a}{T_0 - T_a}\right)$ is a good measure of the progress of cooling. If this quotient Q is <0.3, only a minimum interval of the time since death should be given. T_0 = rectal temperature at death ($T = 0$), T_r = rectal temperature at any time, T_a = ambient temperature

A could be empirically identified on the material studied under standard conditions. The material described by De Saram et al. [10] and re-evaluated by Henssge [13, 14, 22] was stated as follows: A is 1.25 for ambient temperatures of ≤23 °C and 1.11 for ambient temperatures of >23 °C.

The temperature at the time of death, T_o, is the third constant of the formula established by Marshall and Hoare [26]. A temperature of 37.2 °C is used for this constant. With this empirical solution of Marshall and Hoare's formula, the time of death can be computed as follows:

$$Q = \frac{T_R - T_a}{37.2 - T_a} = 1.25 \times \exp(B \times t) - 0.25 \times \exp(5 \times B \times t)$$

for ambient temperatures of ≤ 23 °C or

$$Q = \frac{T_R - T_a}{37.2 - T_a} = 1.11 \times \exp(B \times t) - 0.11 \times \exp(10 \times B \times t)$$

for ambient temperatures of >23 °C using computer programs developed by Henssge [13, 14, 22] or a nomogram (Fig. 4).

The nomogram is valid for the chosen standard conditions of cooling (naked body with dry surfaces, lying extended on a thermally indifferent base, in still air). Conditions that accelerate or delay body cooling compared with standard conditions (e.g., lying in water; wind on one hand, while the other hand is covered; wearing clothing) reduce or increase the real body weight. Extensive cooling experiments under various cooling conditions led to empirically determined corrective factors for body weight (Table 9). With these corrective factors, the nomogram can be used for non-standard cases. The corrective factors themselves are dependent on body weight (Table 10) in cases of a low or high body weight under higher thermic insulation conditions [11, 22]. Higher body weights require the use of lower factors, and lower weights require higher factors. The nomogram can also be used in cases of sudden change in ambient temperature.

Application of the nomogram method in casework requires that the following steps be taken:

1. Inspection of the crime scene, including body posture; clothing; covering; exposure of the body to sunshine,

Table 9 Empirical corrective factors for body weight

Dry clothing/covering	Air	Corrective factor	Wet through clothing/covering wet body surface	In air	In water
		0.35	Naked		Flowing
		0.5	Naked		Still
		0.7	Naked	Moving	
		0.7	1–2 thin layers	Moving	
Naked	Moving	0.75			
1–2 thin layers	Moving	0.9	≥2 thicker layers	Moving	
Naked	Still	1.0			
1–2 thin layers	Still	1.1	2 thicker layers	Still	
2–3 thin layers		1.2	>2 thicker layers	Still	
1–2 thicker layers	Moving or still	1.2			
3–4 thin layers		1.3			
More thin/thicker layers	Without influence	1.4			
		…			
Thick blanket		1.8			
		…			
+		2.4			
		…			
Clothing combined		2.8			

The listed values for each corrective factor (c.f.) apply to bodies of average weight (reference, 70 kg; see Table 10) in an extended position on a thermally indifferent supporting base

"Thermally indifferent" supporting bases include usual floors of rooms, dry soil, lawn, and asphalt. In comparison, bases that appear more thermally insulating/heat conducting should additionally be taken into account

Excessively thickly upholstered bases require a c.f. of 1.3 for naked bodies. For clothed bodies, the c.f. should be increased by 0.1 units (thickly clothed) to 0.3 units (very thickly clothed)

Insulating but not excessively thickly upholstered bases such as a mattress (bed) or thick carpet require a c.f. of 1.1–1.2 for naked bodies

Bases that accelerate cooling, such as concrete or stony or tiled bases on ground, require a c.f. of up to 0.75 for naked bodies

For clothed bodies lying on bases, the c.f. should be reduced by 0.1 units (thicker clothes) or 0.2 units (very thin clothes)

Table 10 Dependence of corrective factors on body weight

Cooling conditions	Real body weight (kg)																	
	4 Average range	6	8	10	20	30	40	50	60	70	80	90	100	110	120	130	140	150
										1.3								
Clothing, more layers	1.6	1.6	1.6	1.6	1.5					1.4					1.3	1.2	1.2	1.2
	2.1	2.1	2.0	2.0	1.9	1.8				1.6				1.4	1.4	1.4	1.3	1.3
Bedspread	2.7	2.7	2.6	2.5	2.3	2.2	2.1	2.0		1.8			1.6	1.6	1.6	1.5	1.4	1.4
	3.5	3.4	3.3	3.2	2.8	2.6	2.4	2.3		2.0		1.8	1.8	1.7	1.6	1.6	1.5	1.5
	4.5	4.3	4.1	3.9	3.4	3.0	2.8	2.6	2.4	2.2	2.1	2.0	1.9	1.8	1.7	1.7	1.6	1.6
Clothing + bedspread	5.7	5.3	5.0	4.8	4.0	3.5	3.2	2.9	2.7	2.4	2.3	2.2	2.1	1.9	1.9	1.8	1.7	1.6
	7.1	6.6	6.2	5.8	4.7	4.0	3.6	3.2	2.9	2.6	2.5	2.3	2.2	2.1	2.0	1.9	1.8	1.7
Feather mattress	8.8	8.1	7.5	7.0	5.5	4.6	3.9	3.5	3.2	2.8	2.7	2.5	2.3	2.2	2.0	1.9	1.8	1.7
	10.9	9.8	8.9	8.3	6.2	5.1	4.3	3.8	3.4	3.0	2.8	2.6	2.4	2.3	2.1	2.0	1.9	1.8

windows (e.g., are they closed or open?), radiators, and floor (e.g., is it thermally indifferent?).

2. Measurement of ambient temperature (air) close to the body and at the same level as the body (10–20 cm above the base) and temperature of the underlying surface; determination of whether thermic conditions have changed since the body was found.
3. Single measurement of deep rectal temperature at the scene using an officially calibrated electronic thermometer with probes for measuring air, surface, and rectal temperature. The deep rectal temperature must be measured at least 8 cm within the anal sphincter.
4. Estimation of body weight; then at autopsy, determination of whether the estimation was correct.
5. Evaluation of corrective factors (i.e., are there any conditions that could have accelerated or delayed cooling compared with standard conditions?). For rectal temperature, relevant factors are thermic conditions of the lower trunk only, such as clothing/covering, resting or moving air, and type of supporting base. In cases of strong insulating conditions and very high or low body weight, a corrective factor must be applied based on the body weight.
6. Use of the nomogram (Figs. 14, 15).

Several investigators (personal communication) have noticed that if they use photocopies of Henssge's nomogram from different textbooks or different editions of the same textbook, they obtain different results using the same data, no matter how carefully the relevant lines were drawn. Obviously, this error was caused by the way the nomogram was typeset in the textbooks. Therefore, photocopies of the nomogram found in textbooks should not be used in practical casework. The nomogram can be downloaded from the homepage of the Institute of Forensic Medicine, University of Bonn (https://www.rechtsmedizin.uni-bonn.de/dienstleistungen/for_Med/todeszeit/; last accessed February 26, 2016). Alternatively, computer programs may be used (e.g., www.amasoft.de/; last accessed February 26, 2016).

To use the nomogram, the points on the scales for rectal and ambient temperature must be connected by a straight line. This line crosses the diagonal at a particular point. Draw a second straight line, going through the center of the circle, from the bottom left of the nomogram and the intersection of the first line and the diagonal. The second line crosses the semicircles that represent body weights. The time of death can be seen at the intersection of the semicircle with the body weight. The second line touches a segment of the outermost semicircle. Here, the permissible variation of 95 % CI can be seen for standard cases or cases using corrective factors. If the ambient temperature or corrective factors are in question, the procedure should be repeated with other appropriate values. If the chosen ranges of ambient temperature and corrective factors are wide, it is recommended that two values of time are used: (1) the shortest time resulting from the combined lower limits of the evaluated ranges of the body weight, ambient temperature, and corrective factor; and (2) the longest time resulting from the upper limits of the body weight, ambient temperature, and corrective factor. The range of the time of death can be determined in this way.

If the rectal temperature has nearly reached the ambient temperature ($Q < 0.3$), only a minimum interval of the time of death should be given (mean value minus appropriate 95 % CI). For temperatures of >23 °C, another nomogram developed based on the data reported by De Saram et al. [10] must be used (Fig. 15). The only difference between this nomogram and the nomogram for temperatures ≤23 °C is the relative duration of the postmortem temperature plateau (shorter duration in higher ambient temperatures). The requirements for use of this nomogram (Figs. 14, 15) are as follows:

- no strong radiation (e.g., sun, heater, cooling system);

- no strong fever or general hypothermia;
- the place of death must be the same as that where the body was found;
- no uncertain severe changes in the cooling conditions during the period between death and examination;
- no high thermal conductivity of the surface underneath the body; and
- no long terminal period after fatal injury (time of death inconsistent with time of assault).

The accuracy of the nomogram method was compared with that of police investigations in a multicenter study (76 cases) and a single-center study (72 cases) [7, 20, 22]. These were rare field studies on the accuracy of the proposed methods. Both studies covered a wide range of ambient temperatures, body weights, and corrective factors. The estimated time of death did not contradict the established time of death in any of the cases. Especially in the earlier stages, the police investigations were supported effectively by the nomogram method.

Cooling conditions can be simulated using cooling dummies [17, 18, 22]. Of all methods developed to estimate the time of death, the nomogram method based on the two exponential terms by Marshall and Hoare [26] is by far the most successful and reliable. This is because the actual cooling conditions could be taken into consideration quantitatively, and data on the precision of the method are available. Additionally, field studies have confirmed the accuracy and reliability of the method.

Practical application of methods for estimating time of death

Because no single method has been shown to produce precise and accurate results, practitioners generally use a combination of methods to derive an estimate. Of all the methods used to estimate the time of death, the nomogram method developed by Henssge [13, 14, 22], based on body cooling after death, is the most intensively investigated and the most precise and reliable. Therefore, it should be used as the leading method in all cases if requirements are met. Even in the most favorable cases, however, the resulting time since death has an interval of ±2.8 hpm around the mean value. Efforts should be made to narrow this range by combining the temperature method with other methods [19, 20, 23]. Methods that can be combined with the nomogram method include the time-dependent criteria of rigor mortis (beginning, maximum, reestablishment), hypostasis (beginning, confluence, maximum, disappearance on thumb pressure, complete/incomplete shifting), electrical excitability of facial muscles (m. orbicularis oculi with 6°, m. orbicularis oris), mechanical excitability of skeletal muscle (idiomuscular pad), and the pharmacologically induced excitability of the iris. The question is how to use the data of these time-dependent classic signs of death and supravital reactions.

The mean value for any criterion of these classic methods does not represent the time frame in which a positive reaction occurs. For reliable estimations derived from these criteria, only their upper or lower limits should be used (Fig. 16). In Fig. 16 the mean values, 95 % CIs (electrical excitability of the orbicularis oculi muscle), or variations (lividity, mechanical excitability, rigor, chemical excitability) of the criteria are arranged chronologically over the time of death (*x*-axis) according to the increasing mean values. As can be seen, the mean value does not represent the time interval during which a positive reaction occurs. Therefore, for reliable estimations derived from these criteria, only the upper or lower CIs for these criteria should be used. Figure 17 shows a chart with all the data for an acutal case, including the signs of death and supravital reactions together with the estimated time of death based on the nomogram. The data are rearranged into a special chart that facilitates selection of the most helpful criteria (Fig. 17).

For casework, estimating the time of death using the nomogram method begins with taking temperatures and choosing the appropriate corrective factor. Depending on the range given by the nomogram method, specific criteria are examined that are suitable for narrowing the upper and lower margins provided by the temperature method. Using this chart at the site of death guarantees that the examination of the body is efficient and comprehensive with respect to estimation of the time of death.

An example is shown in Fig. 18. At the crime scene, the examination began with measuring the rectal temperature. Using the nomogram, the estimated time since death ranged from 4.5 hpm (lower limit) to 10.1 hpm (upper limit). The lower limit could be increased only by a value of >4.5 hpm, and the upper limit could be reduced only with a value of <10.1 hpm. The electrical excitability of facial muscles showed a positive reaction according to degree IV, which means that time since death was <8 hpm. Furthermore, rigor mortis was reestablished after it was broken, which can be observed only up to 8 hpm. Therefore, the upper limit of the estimated time since death (10.1 hpm) could be reduced to 8 hpm.

When temperature methods cannot be used alone (e.g., hypothermia, fire in the building where the bodies were found), valuable information on the time since death can be obtained using this chart. In the case shown in Fig. 19, the temperature-based-nomogram-method revealed an estimated time since death of 8.8–14.3 hpm according to a rectal temperature of 26.6 °C, ambient temperature of 10 °C, and body weight of 72 kg. Rigor mortis had not yet started, and electrical excitability showed a full reaction

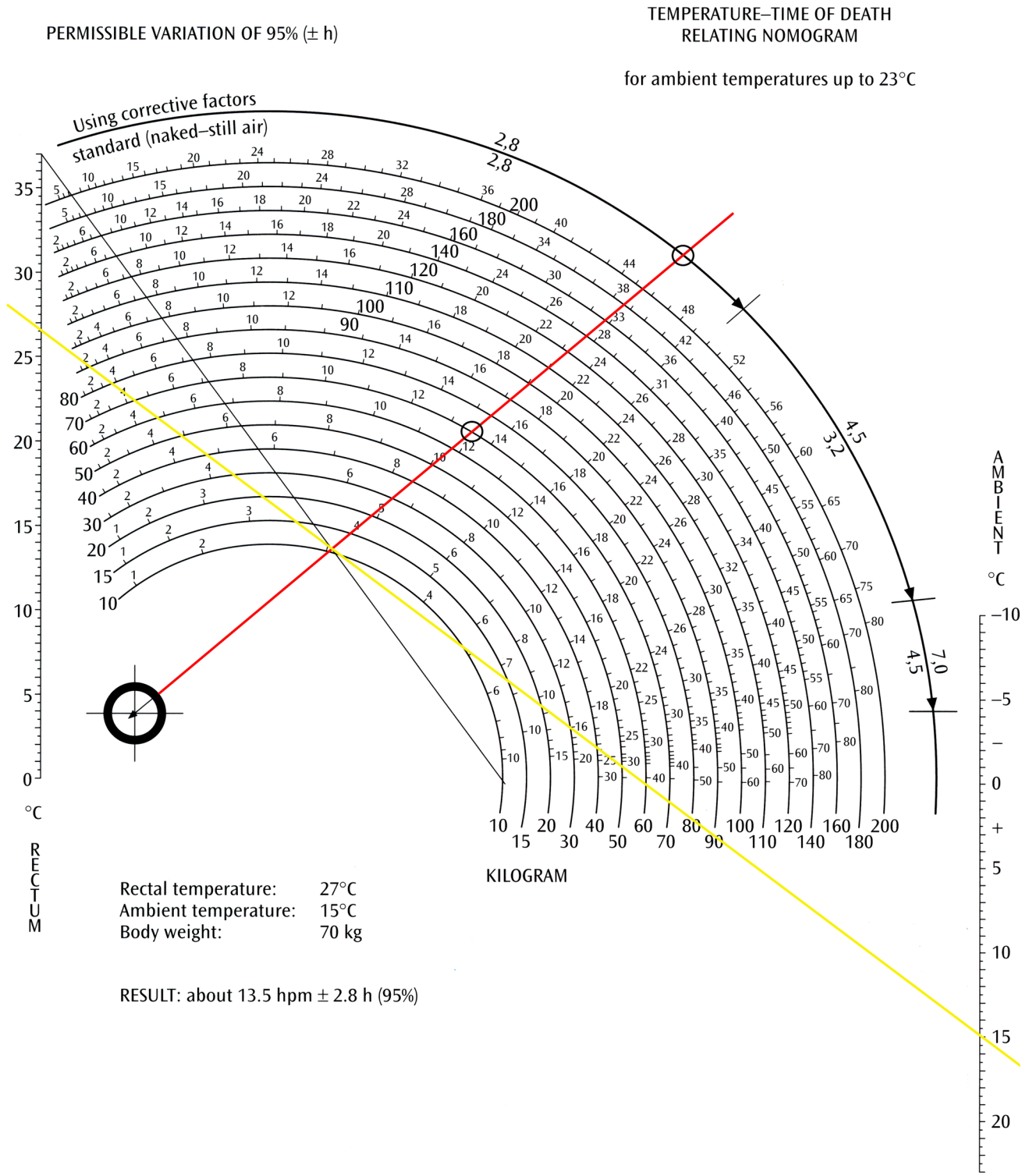

Fig. 14 Temperature–time of death nomogram for ambient temperatures up to 23 °C. At the scene of a crime, for instance, a rectal temperature of 27 °C at an ambient temperature of 15 °C was measured. First, the points of the measured rectal temperature and ambient temperature are joined by a *straight line* (*yellow*) that crosses the diagonal of the nomogram at a specific point. A second straight line is then drawn passing through the *center of the circle* (*below left* of the nomogram) and the intersection of the first line and the diagonal (*red line*). The second line crosses the semicircles for different body weights. The time since death (in this case, for a 70-kg body weight) can be read at the intersection of the semicircle of the given body weight. The intersection gives the mean time since death, and the intersection with the outer circle gives the 95 % limit of confidence, which may be higher if corrective factors must be used

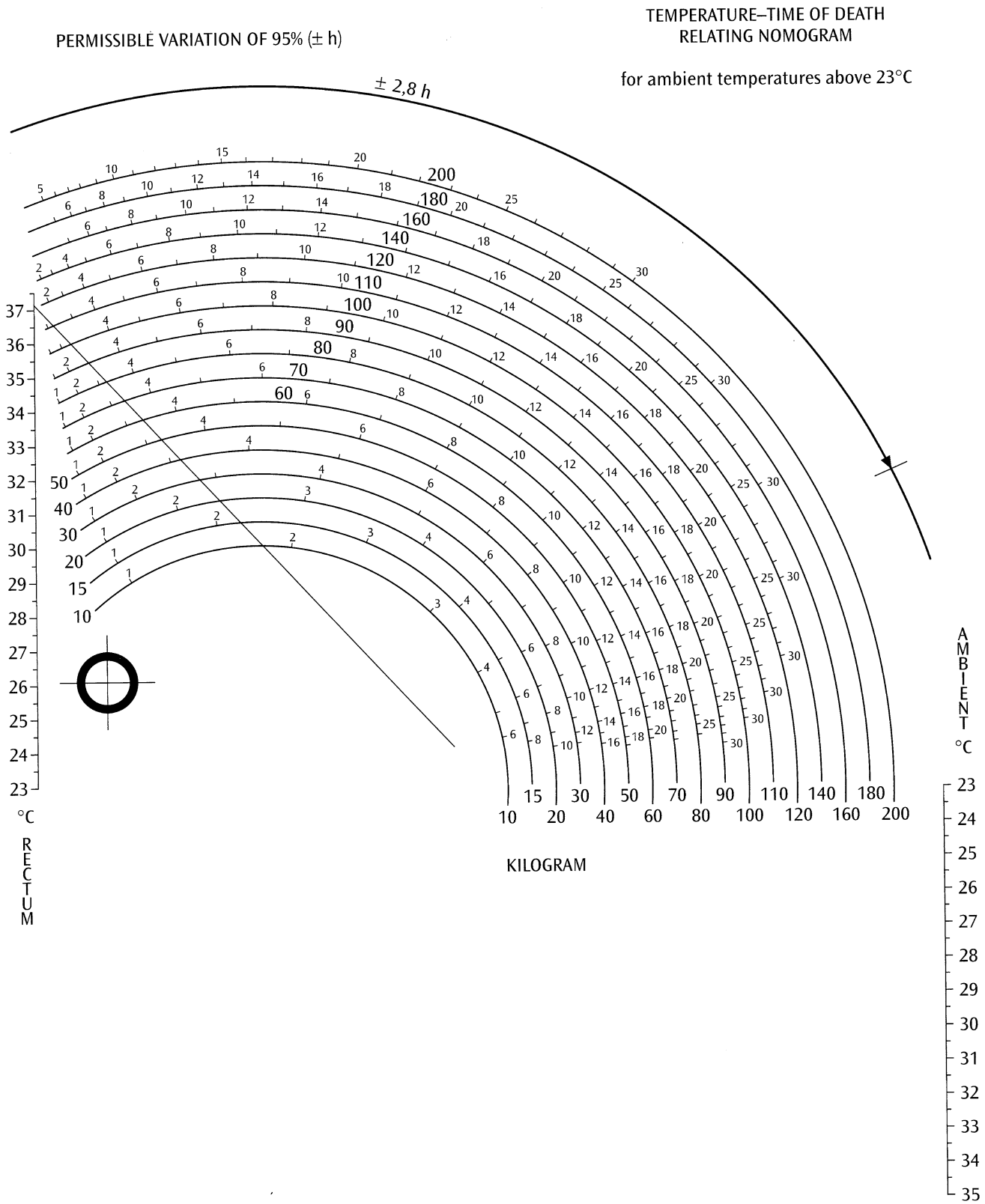

Fig. 15 Temperature–time of death nomogram for ambient temperatures of >23 °C

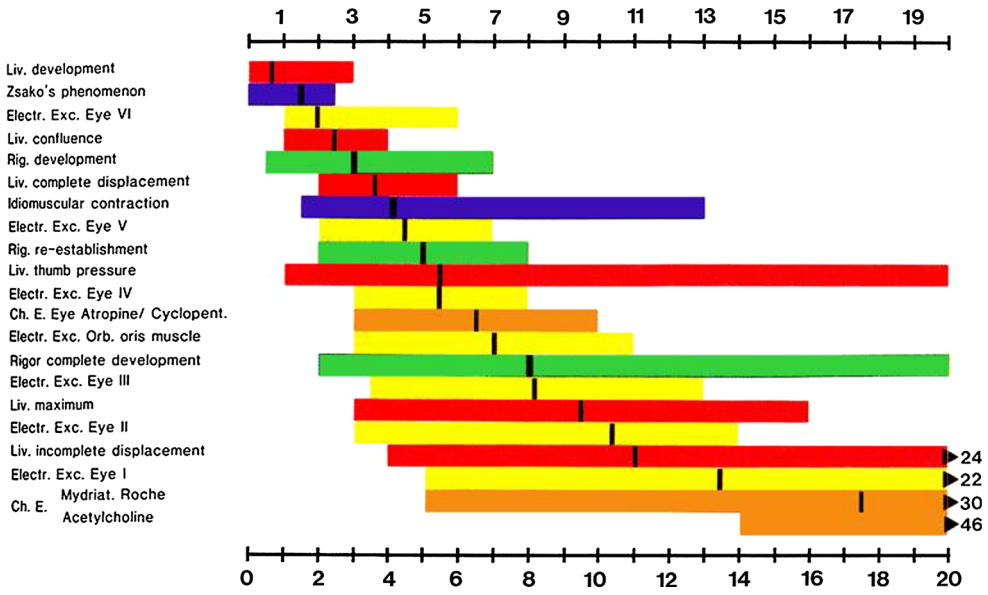

Fig. 16 Mean values (*black bars*) and variations of different criteria depending on time of death. *Red* lividity; *blue* mechanical excitability of skeletal muscle; *yellow* electrical excitability; *green* rigor mortis; *orange* pharmacological excitability

(degree VI), resulting in an estimated time since death at less than 6 or 7 hpm. These results were not in agreement. Autopsy revealed hypothermia as the cause of death, and the hypothermia-induced decrease in the body temperature during life simulated the longer time since death. Thus, body temperature must not be used to estimate the time since death in cases of fatal hypothermia; instead, other parameters give reliable results.

Our own experience using electrical excitability in addition to the nomogram method revealed that, especially during the time interval of 3–8 hpm, the combination of the two methods resulted in a more precise time of death estimate than either method alone (Fig. 20). Disparate results between the estimated time of death derived from the degree of electrical excitability and the nomogram may indicate the need to delve further into special circumstances leading to death (e.g., hypothermia).

A recent field study using a combined method on 72 consecutive cases over a long-lasting PMI revealed that the estimation of the time since death using the temperature method was made more precise using non-temperature methods in 49 cases. The degree of electrical excitability was the most valuable additional method, but classic signs may also improve the nomogram results. Even if the temperature-based results are not made more precise, but only confirmed by these means, the investigators' confidence in their opinions and statements regarding the time of death may increase because they can base their expert evidence on independent methods.

Biermann and Potente [105] and Potente [106] described an interesting development using a combined method. Their method was based on a conditional probability distribution that can be calculated if non-temperature-based findings are taken into account. It ensures that the probability inside the interval is 95.45 %. The method was successfully applied to 54 cases and decreased the interval by >15 %.

Additional methods

Potassium in vitreous humor

Most chemical methods of estimating time since death measure concentration changes (increases or decreases) in various fluid compartments. For example, autolysis results in increased potassium and decreased sodium and chloride in the extracellular fluid compartment. Some of these autolysis-induced concentration changes are combined with changes resulting from metabolic processes, such as increased ammonia, lactic acid, and hypoxanthine or decreased glucose. Metabolic and autolytic processes are influenced by the temperature, disease, duration of the terminal phase before death, and site and method of sample acquisition. The resulting inter-individual variation is so great that the concentration changes are of no value in practice.

Autolysis proceeds more rapidly in blood than in cerebrospinal fluid (CSF) and more slowly in vitreous humor (VH) (because of its isolated and confined topography) than in CSF. Thus, CSF and VH are the most extensively studied fluid compartments (the speed and direction of change in blood was recognized as being largely unpredictable as much as six decades ago). Concentration gradients after loss of selective membrane permeability disappear in blood within a few hours after death, in CSF within 15–20 hpm, and in VH after 120 hpm. Therefore, VH is the main fluid compartment studied to investigate late postmortem chemical changes.

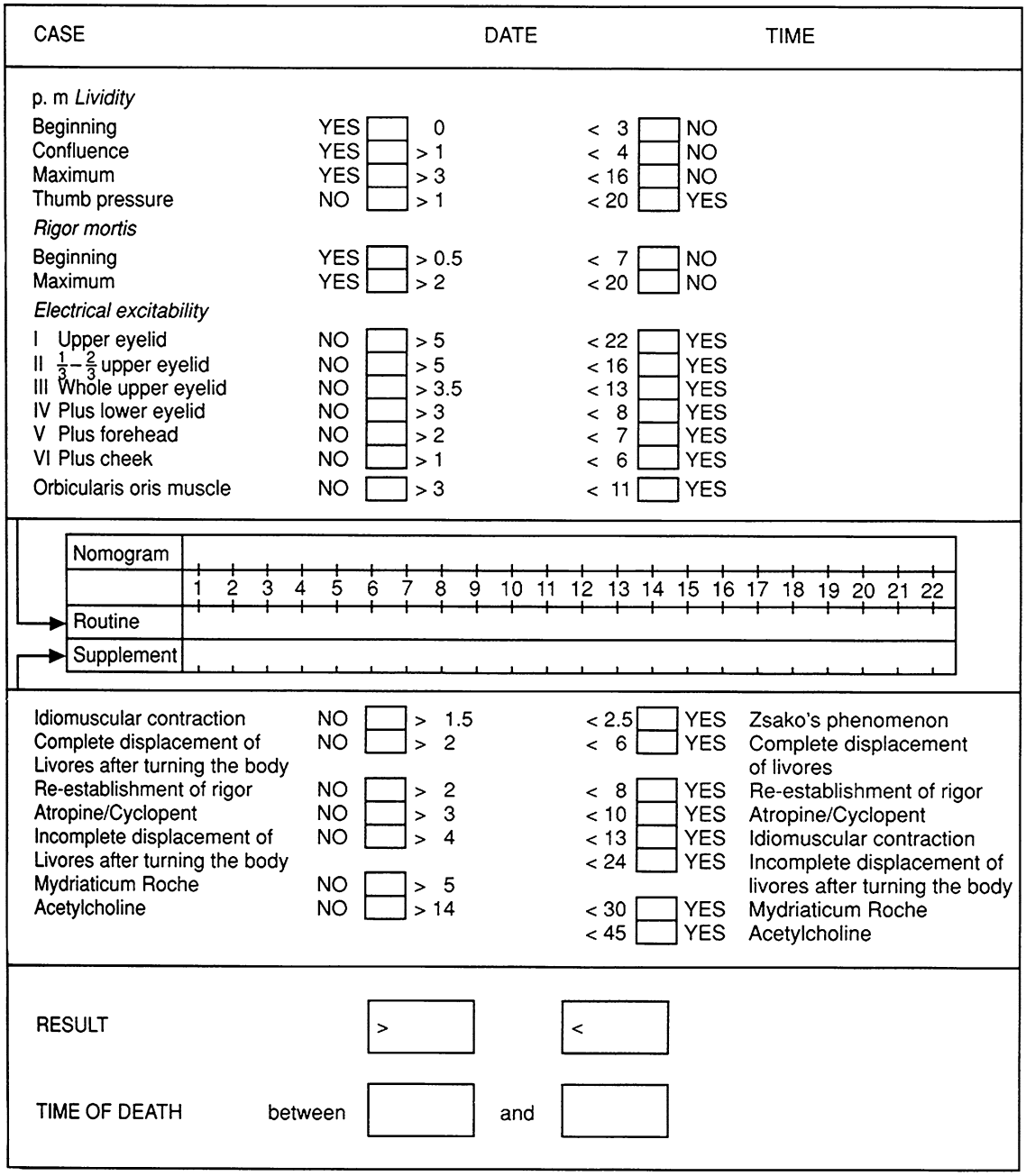

Fig. 17 Integrating chart for casework at the scene of a crime

The postmortem increase in the potassium concentration in VH, first described by Sturner [83] and further discussed by Sturner and Gantner [84], is the most extensively studied parameter for estimating the PMI (Table 11). Factors governing the postmortem rise of VH potassium (i.e., temperature, chronic illness, and urea retention) and the range of scatter are known and can be taken partly into consideration. Data on the precision of the method are available. After the original description by Sturner [83], subsequent authors found a much wider range of scatter, especially when cases with abnormal electrolytes prior to death were included. Thus, various statistical parameters of the regression line were described [57–68, 72, 77, 78, 87, 88]. The slope of Sturner's formula is one of the flattest reported in the literature. It should therefore be used only if the environmental temperature during the PMI was close to refrigerator levels. The slope increases with increasing ambient temperature, as shown experimentally by Rognum et al. [80], Zilg et al. [87], and Zilg [88]. When different formulas for estimating the time of death are compared, reliable results are achieved with the formulas described by Madea et al. [67, 68] and Munoz et al. [77, 78] for climates in Central Europe.

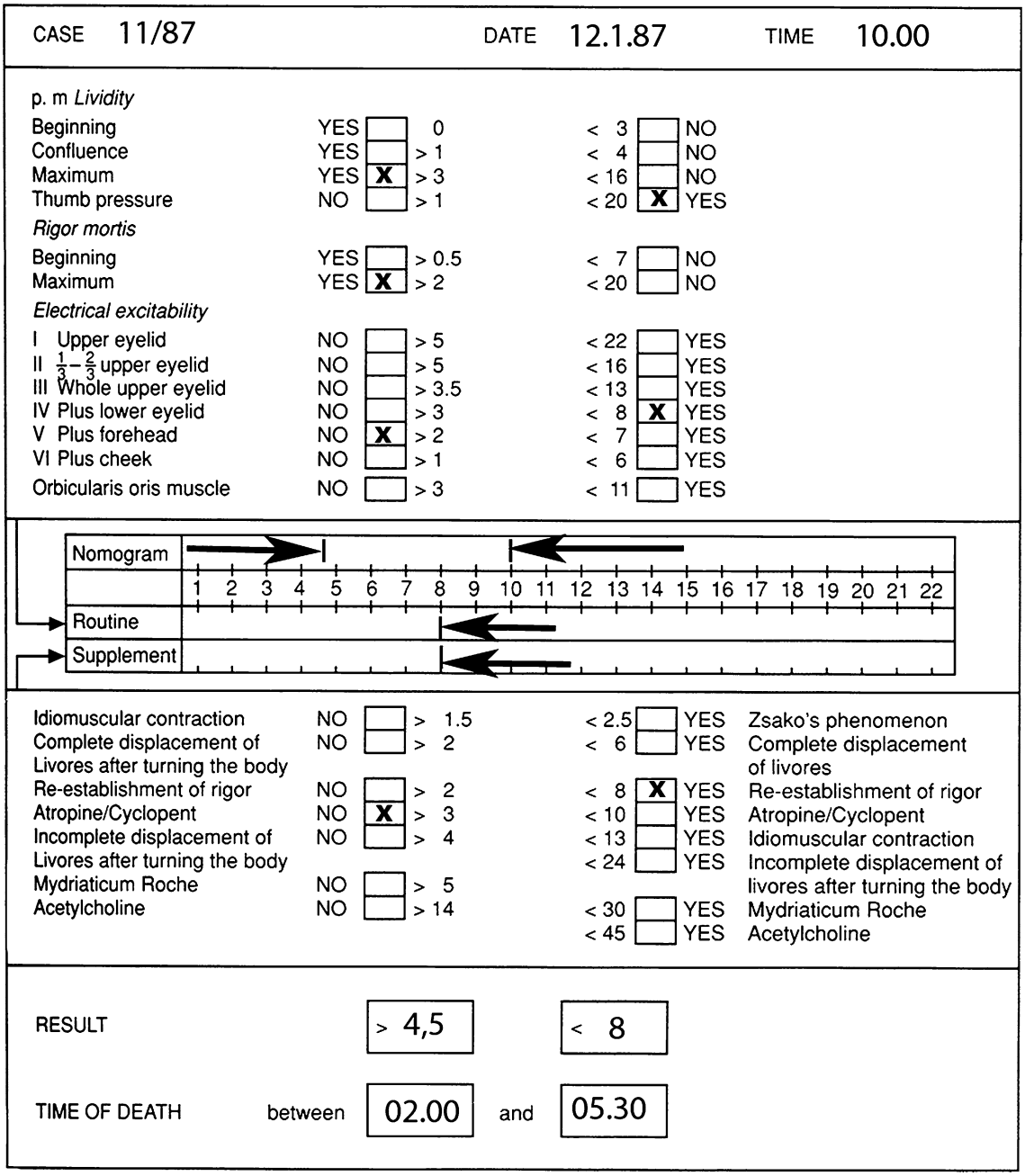

Fig. 18 Integrating chart for casework at the scene of a crime with an example

Although there is a large amount of literature on the VH potassium concentration, it is rarely used in practice or as evidence in court cases. The formula developed by Zilg et al. [87], taking into account the ambient temperature, may be helpful to distinguish whether death occurred within the past few (2–3) days or more than 1 week ago.

Urea as inner standard

A second factor, other than temperature, that determines the increase and scatter of VH potassium is the patient's state of health or the presence of a chronic illness preceding death. Potassium concentrations in individuals who have died after a chronic illness are much more erratic than those of individuals who have died of acute trauma [63, 73]. Additionally, the slopes of the potassium increases are much steeper in individuals with significant urea nitrogen retention (>100 mg/dl) (Table 12). In an entire sample that included clinical and forensic pathology cases, the 95 % CIs were ±34 h. By eliminating cases with urea values of >100 mg/dl and, in a second step, adding cases with a terminal episode of >6 h, the 95 % CIs could be reduced to ±22 and ±20 h, respectively.

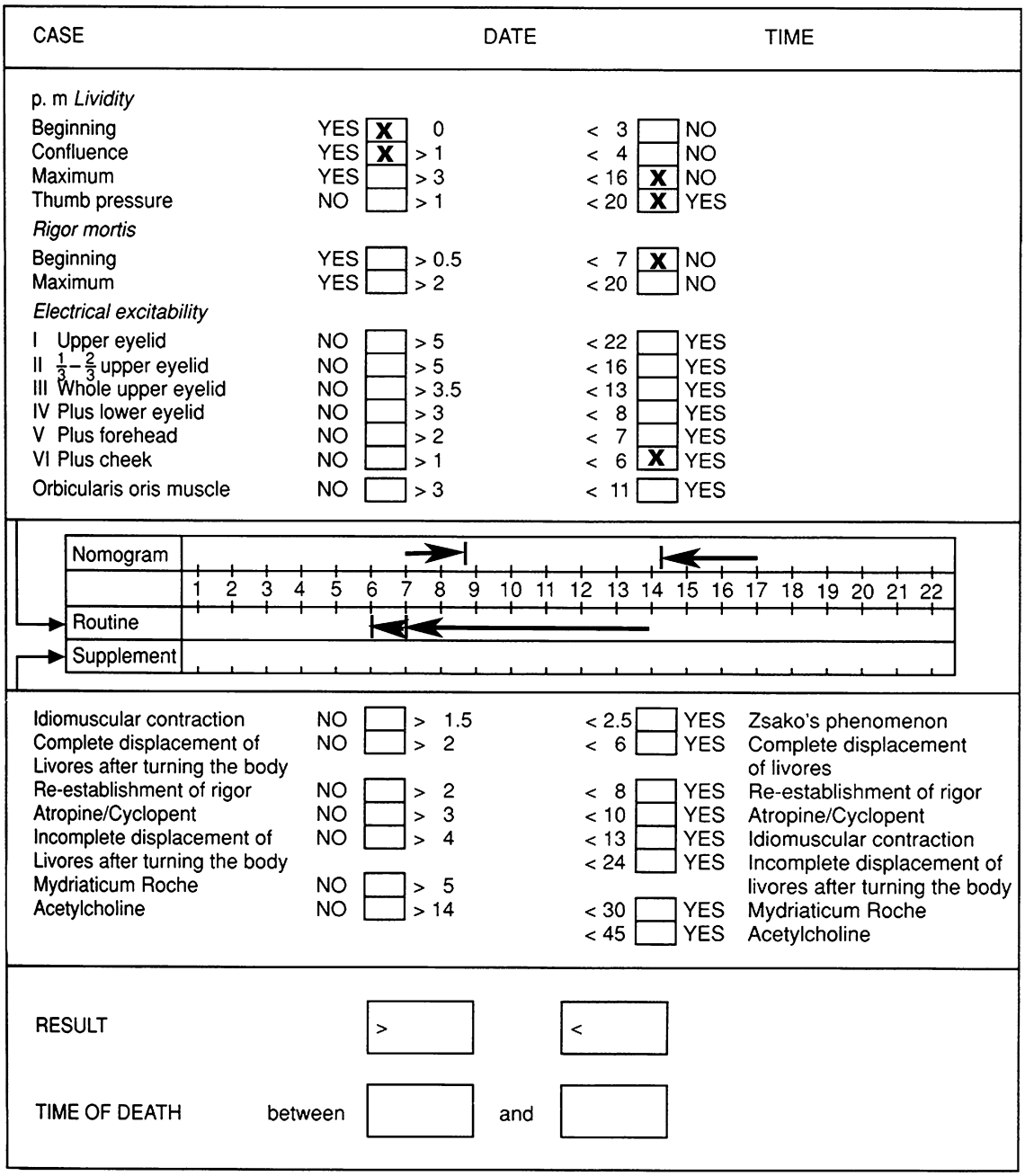

Fig. 19 Integrating chart with contradictory results of death time estimation based on body cooling (nomogram), rigor mortis, and electrical excitability (case of fatal hypothermia)

The VH urea nitrogen concentration is therefore a suitable indicator of disturbed homeostasis of electrolyte metabolism and, depending on the urea values, the corresponding reference samples and formula can be chosen to extrapolate the time of death with different 95 % CIs. The correlation of the precision of death time estimation with inner standards as critical levels of urea and/or creatinine has been confirmed by independent authors [60].

Dependent versus independent variables

Munoz et al. [78] recommended against using the PMI as the independent variable and potassium as the dependent variable. Instead, they suggested that potassium should be the independent variable to estimate the PMI. In their opinion, using the PMI as the independent variable leads to false estimates. By changing the variables, a new formula is obtained in which potassium is considered the

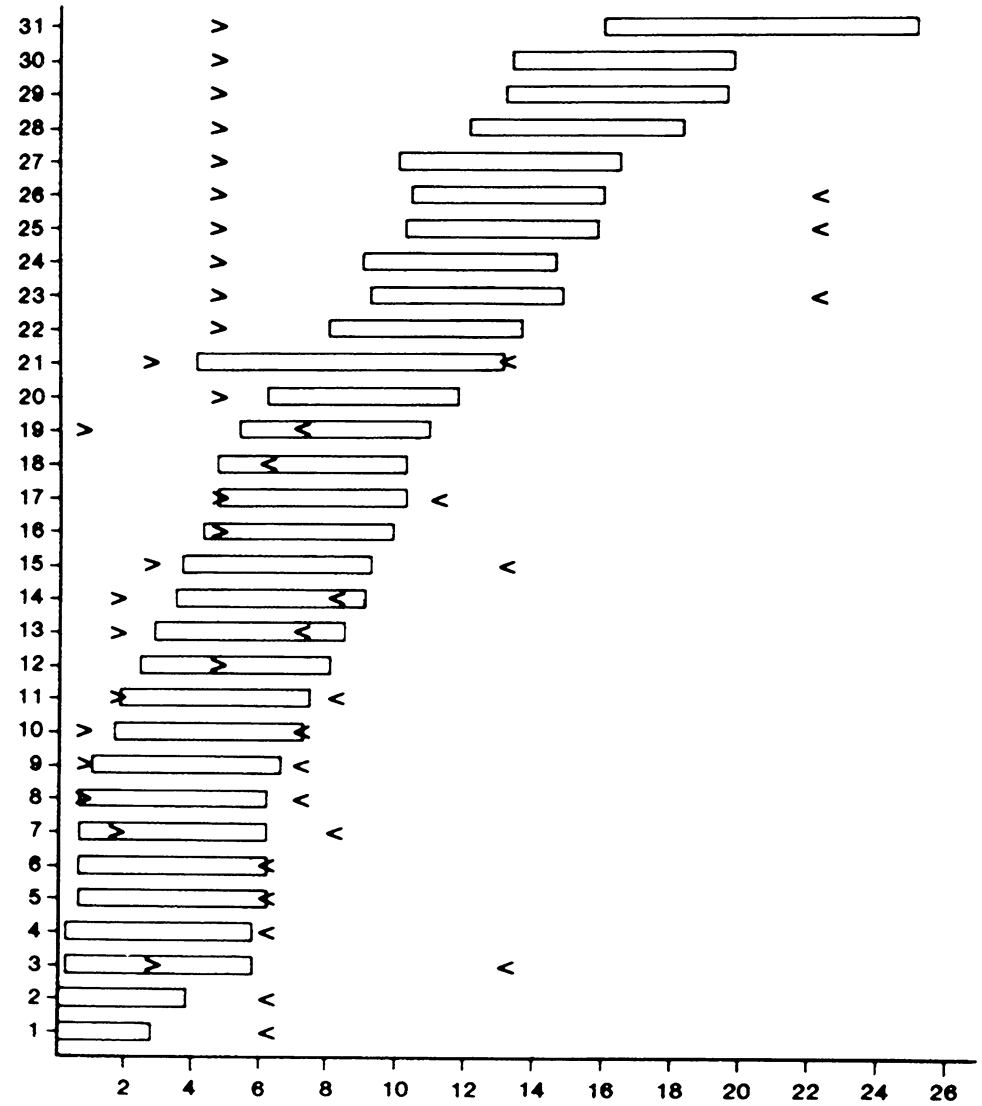

Fig. 20 Combined application of the temperature-based nomogram and the electrical excitability for determining the time since death. *y*-axis: case numbers. *Boxes* death time estimation by the nomogram method (lower and upper 95 % limits of confidence).><: death time estimation based on the degree of electrical excitability. For instance, degree III positivity (Case 15) not only provides the information that the time since death is <13 hpm but also indicates degree IV negativity and therefore that the time since death is >3 hpm. Especially during the time period from 3 to 8 hpm, combining electrical excitability with the nomogram method allows more precise death time estimation than using one method alone. The real time since death is always within the calculated time since death

independent variable and the PMI is considered the dependent variable, which makes the estimated time of death more precise. This statistical approach led to a more precise estimated time of death, which we confirmed on our own material. With potassium as the independent variable, the accuracy of the estimated time since death with 95 % CI was ±23.27 hpm (i.e., more precise than ±25.96 hpm using potassium as the dependent variable, with a time interval of up to 130 hpm). The difference in precision, however, was not statistically significant.

Loess procedure

Lange et al. [66] reanalyzed the data of six studies on the rise of vitreous potassium comprising a total of 790 cases. This reanalysis revealed that the relationship between VH potassium and PMI is not completely linear and that the residual variability of VH potassium as a function of PMI is not constant. Therefore, they developed a new approach for modeling VH potassium and PMI that accommodates nonlinearities and changing residual variability. First, a local regression model—specifically, a Loess smooth curve—was

Table 11 Equations for the increase in potassium in vitreous humor

Reference	Equation (PMI given in h)	*N*	Max PMI (h)	Comments
Adelson et al. [57]	PMI = 5.88 [K^+] − 31.53	209	21	–
Sturner and Gantner [84]	PMI = 7.14 [K^+] − 39.1	125	104	–
Hanson et al. [62]	PMI = 5.88 [K^+] − 47.1	203	310	–
Coe [60]	PMI = 6.15 [K^+] − 38.1	145	100	A separate equation was provided for a PMI of <6 h
Stephens and Richards [82]	PMI = 4.20 [K^+] − 26.65	1427	35	Outliers, drownings, SIDS, electrolyte imbalances, and temperature extremes were excluded
Madea et al. [67]	PMI = 5.26 [K^+] − 30.9	107	130	Cases involving elevated urea and prolonged agony were excluded
James et al. [63]	PMI = 4.32 [K^+] − 18.35	100	80	Also included hypoxanthine
Munoz et al. [77]	PMI = 3.92 [K^+] − 19.04	133	40	Only non-hospital cases were examined; there was a change in variables
Zhou et al. [86]	PMI = 5.88 [K^+] − 32.71	62	27	–
Jashnani et al. [64]	PMI = 1.076 [K^+] − 2.81	120	50	Mostly included cases involving sepsis or tuberculosis
Bortolotti et al. [59]	PMI = 5.77 [K^+] − 13.28	164	110	–
Mihailovic et al. [76]	PMI = 2.749 [K^+] − 11.98	32	30	Repetitive sampling
Siddamsetty et al. [81]	PMI = 4.701 [K^+] − 29.06	210	170	–
Zilg et al. [87]	$\mathrm{PMI} = \frac{\ln\left(\frac{M-C}{M-[K^+]}\right)}{L_0+m_A A+m_T T}$	462	409	No cases were excluded; the proposed equation includes temperature and patient age

PMI postmortem interval, *SIDS* sudden infant death syndrome

Table 12 Precision of time of death estimation using vitreous potassium concentration in different random samples

	Urea as inner standard		
	Entire sample	Urea < 100 mg/dl	Change (%)
n	270 (170)	288 (138)	−15.5
Intercept	6.10 (5.99)	6.02 (5.88)	−1.3
Slope	0.20 (0.2033)	0.18 (0.1877)	−10.0
Correlation coefficient	0.89 (0.86)	0.91 (0.89)	+2.2
Variance s^2	8.57	5.09	−40.6
Standard deviation S_{yx}	2.93 (3.42)	2.25 (2.62)	−23.2
95 % limits of confidence (h)	±25.51 (± 34)	±21.78 (± 22)	−14.6

Urea was used as the inner standard. Statistical parameters of the entire sample and subgroups are given. The data in brackets are from Madea et al. [67]

fitted separately to the data from each of the six studies. The data of all six studies were then combined to yield a single Loess curve with 95 % CI (Fig. 21). The estimated Loess curve and CI were then used in an inverse prediction method to construct low, middle, and high PMI estimates at given VH potassium concentrations (Table 13).

The reliability of the estimated PMI decreased with increasing potassium concentration. According to the authors, however, the PMI estimates were more precise over the entire range of VH potassium and PMI than those obtained from any single study. For potassium concentrations of <7 mmol/l, the extent of the lower and upper 95 % CIs was ±1 hpm. For potassium concentrations of >7 but <12 mmol/l, the extent of these confidence limits was ±2 hpm. For potassium concentrations of >12 and <18 mmol/l, the extent was ±3 hpm, whereas that for >18 mmol/l was ±5 hpm. For concentrations of >18 mmol/l, the extent was even greater. If these data were reliable, no one would go to a crime scene to estimate time of death—they would simply wait for the autopsy and rely on the VH potassium concentrations.

Because of the much greater variability in the single potassium concentrations of the included studies from the single Loess curve with its 95 % CIs, the reliability of the statistical evaluation remains unclear. In our own cases, we

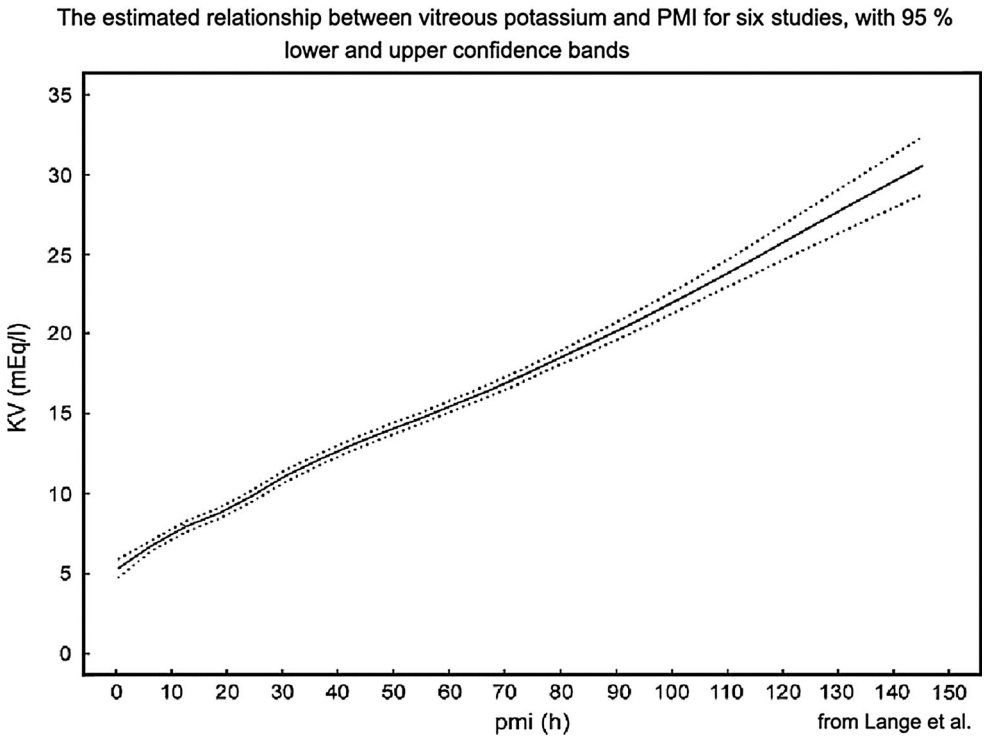

Fig. 21 Estimated relationship between vitreous potassium and postmortem interval for six studies, with 95 % lower and upper confidence bands

could not confirm the precision of the estimated time of death based on this statistical approach, obtaining a high rate of false estimations [72, 73]. Therefore, use of the data in Table 13 is not recommended.

Multiple linear regression analysis

Multiple linear regression analysis uses, in addition to VH potassium, other time-dependent changes in VH analytes [73]. Using a multiple linear regression formula, a 95 % CI of ±14.0 hpm could be achieved when taking potassium, sodium, urea, and glucose into account compared with a 95 % CI of ±16.2 hpm using potassium alone on the same sample. Therefore, it can be concluded that a slight increase in the precision of the estimated time of death can be achieved using multiple linear regression analysis. Measuring VH analytes (potassium, NH_4, Na, and Ba) by capillary zone electrophoresis and taking all ions into account results in an estimated time of death with five-fold higher precision than that obtained using vitreous potassium.

Hypoxanthine in VH

In addition to potassium, measurement of hypoxanthine (Hx) concentration was proposed as a biochemical method for estimating the PMI. A study by Rognum et al. [80] revealed (1) a linear increase in the concentration of Hx in VH during a PMI of up to 120 hpm; (2) dependence of the slope of the increased VH Hx concentration on temperature (the higher the ambient temperature, the steeper the slope); (3) a strong correlation between the VH Hx and VH potassium concentrations; and (4) a smaller range of scatter of the VH Hx than VH potassium concentrations.

Further studies [69, 73] (Table 14), however, confirmed the postmortem increase in the Hx concentration, but the correlation of the potassium concentration with the time of death was found to be much stronger than that of the Hx concentration. Therefore, the estimated time of death was more precise using VH potassium than using VH Hx. This is because the postmortem rise of VH potassium is mainly due to diffusion from the retina into the center of the globe, whereas Hx is a postmortem degradation product of adenine nucleotide metabolism. Hx, formed by several enzymatic reactions, diffuses along the concentration gradient. In theory, it might be expected that a parameter such as a postmortem increase that is solely due to diffusion would correlate more strongly with the time of death than would a parameter that increases because of vital/postmortem degradation and diffusion. The higher precision of the time of death estimated by VH potassium compared with that estimated by VH Hx also becomes apparent from data published by Munoz et al. [78].

Synovial fluid

Synovial fluid is a thoroughly investigated fluid compartment in rheumatology, and handbooks of joint fluid analysis are available. However, only a few studies of

Table 13 Estimated values of postmortem interval for various increasing potassium concentrations in the vitreous humor obtained by combining all 790 cases and using the Loess procedure

Measured vitreous potassium concentration (mml/l)	Estimated postmortem interval (h)		
	Lower 95 % value	Mean value	Upper 95 % value
5.9	2	3	4
6.4	3	5	6
7.0	6	7	8
7.5	8	10	12
8.0	11	13	15
8.5	14	16	19
9.1	18	21	22
10.1	23	25	27
11.1	29	30	32
12.1	33	35	38
13.0	39	41	44
13.9	44	47	50
14.9	51	54	57
15.9	58	61	64
17.0	66	69	72
18.3	74	77	81
19.7	81	85	90
21.1	89	94	100
22.6	98	103	111
24.2	106	113	123

From Lange et al. [66]

medicolegal interest regarding synovial fluid have dealt with alcohol concentration, drug distribution, and postmortem chemistry with a focus on determining cause of death. Our own study on postmortem biochemical examination of synovial fluid revealed that it can be used as a postmortem examination tool [70]. The spread of values was comparable in all examined electrolytes. Evaluation of the data with regard to the time course over the postmortem period was not useful except for glucose and potassium. Especially, the changes in the potassium concentration over time are nearly identical in synovial fluid and VH, which may be of importance if VH is not available.

Decomposition: H magnetic resonance spectroscopy

When putrefactive changes are apparent, only a rough estimation of the PMI is possible based on subjective experience of the forensic pathologist, not by a scientific method. About three decades ago, extensive experimental work was carried out on protein degradation during putrefaction of various organs (e.g., the brain by Bonte [52] and Daldrup [108]). Daldrup proposed a method for calculating the time of death based on amino acid concentrations in the brain. None of these methods, however, gained practical relevance.

Methods developed in radiology, such as H magnetic resonance spectroscopy (H MRS), have recently been applied to identify metabolites emerging during decomposition of brain tissue as a step toward quantitative determination of the PMI during putrefaction. The leading research group in this area is the collaborative group of the Institute of Forensic Medicine and Department of Clinical Research (MR Spectroscopy and Methodology) at the University of Bern [53].

H MRS allows for in situ noninvasive chemical analysis that can be performed using magnetic resonance imaging equipment. Because brain tissue shows small interindividual metabolic variations and is protected from environmental influences by the skull, decay and the appearance of metabolites are expected to follow a reproducible timeframe [53].

The authors in Bern studied eight sheep heads as a model system supplemented by selected human cases. The sheep heads were kept in a closed plastic container after slaughter and stored at a constant temperature (21° ± 3 °C) for 18 days. They were then studied daily for up to 18 days postmortem. In addition, brain samples were obtained at the end of the study and investigated by high-resolution nuclear magnetic resonance to identify unknown

Table 14 Formulae for determining postmortem interval (h) with hypoxanthine (μmol/l)

Reference	Equation obtained*	Formula proposed
Rognum et al. [80]	$y = 4.2x + 7.6$ at 5 °c	
	$y = 5.1x + 7.6$ at 10 °c	
	$y = 6.2x + 7.6$ at 15 °c	
	$y = 8.8x + 7.6$ at 23 °c	
Madea et al. [73]	$y = 1.29x + 3.69$	
James et al. [63]	$y = 3.2x - 0.15$	PMI = 0.31 [Hx] + 0.05
Munoz et al. [77]	$y = 3.01x + 26.45$	PMI = 7.14 [Hx] + 0.17

* y is hypoxhanthine; Variable x is the postmortem interval (h)

Hx hypoxanthine; *PMI* postmortem interval

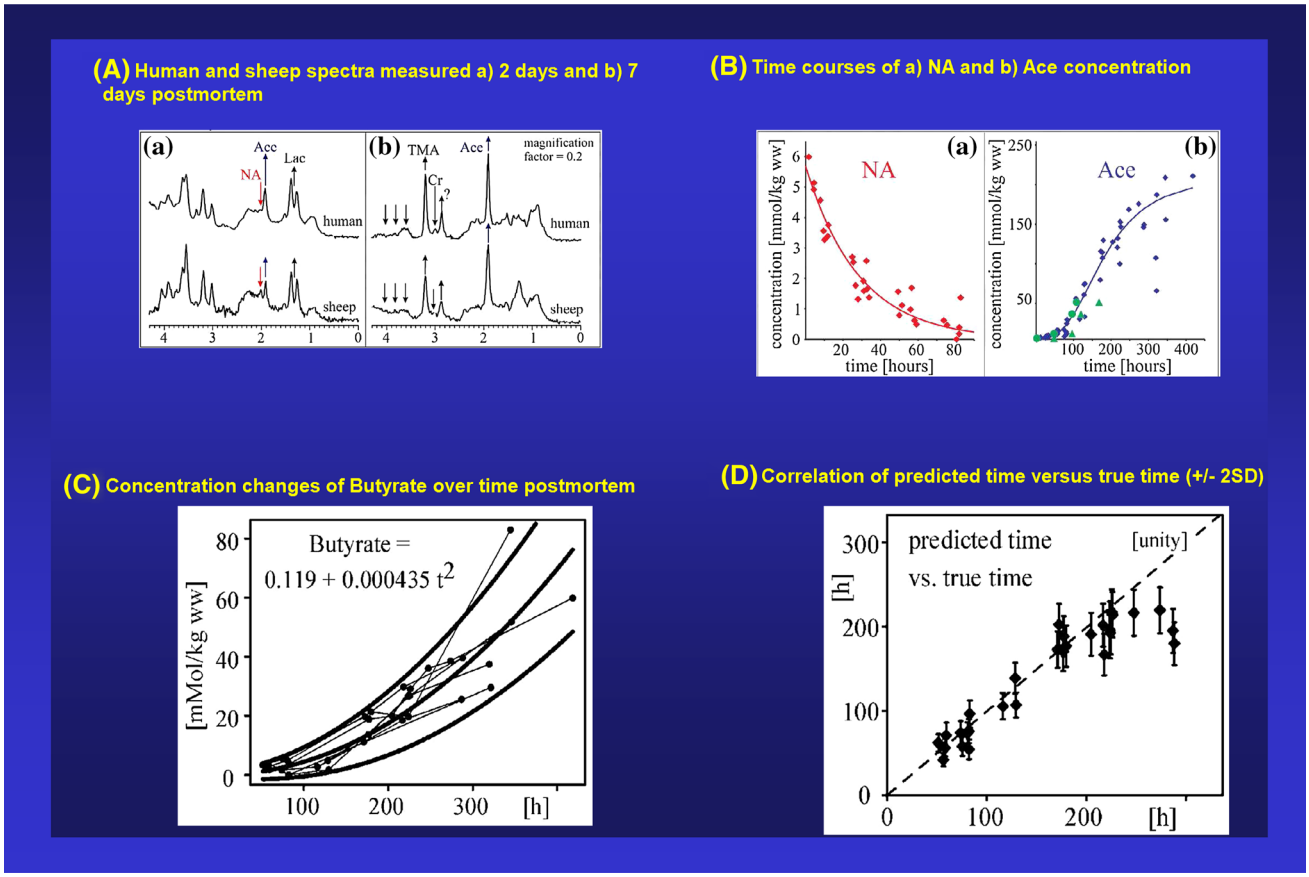

Fig. 22 **A** Human and sheep spectra measured *a* 2 days and *b* 7 days postmortem. **B** Time course of *a* N-acetylaspartate (NA) and *b* Acetate (Ace) concentration. **C** Concentration changes of butyrate over time postmortem. **D** Correlation of predicted time versus actual time (±2SD). Lac, lactate; TMA, trimethylammonium. **A**, **B** from Ith M, Kreis R, Scheuerer E, Dirnhofer R, Boesch C, Using ^{1}H-MR spectroscopy in forensic medicine to estimate the postmortem interval: a pilot study in an animal model and its application to human brain. *Proc Int Soc Magn Reson Med* 2001; 9: 388; **C** and **D** from Scheuerer E, Ith M, Dietrich D, Kreis R, Hueseler J, Dirnhofer R, Boesch C. Statistical evaluation of time-dependent metabolite concentrations: estimation of postmortem intervals based on in situ ^{1}H-MRS of the brain. *NMR Biomed* 2005; 18: 163–172. These figures were reproduced with the permission of the authors and the International Society for Magnetic Resonance in Medicine

metabolites. This method quantifies metabolite concentrations as low as 1 mmol. Brain decomposition resulted in reproducible changes in the concentrations of known metabolites and the appearance of decay products that had to be characterized first. In total, 30 metabolites were identified and quantified in the decomposing brain tissue, 19 of which showed well-defined time courses (Fig. 22A).

For instance, the neuronal marker *N*-acetylaspartate decreased rapidly after death and may serve as an indicator for a time period of <70 hpm (Fig. 22B). Butyrate or propionate, thought to arise from bacterial metabolism, started to increase after 30–50 hpm and exhibited unequivocal function up to 400 hpm (Fig. 22C). Figure 22D compares time predictions for every measurement of the series for five metabolites (acetate, alanine, trimethylamine, butyrate, and propionate), weighted according to their variances with true times after death. The correlation coefficient of the predicted time versus true time was $r = 0.93$ for the whole time period up to 300 hpm. Values are shown with an error range of 2 standard deviations. Figure 22D shows that PMIs of >250 hpm are systematically underestimated in this model system.

As could be expected, comparison of the sheep brain spectra with selected human postmortem cases shows the same metabolites and the same characteristics of appearance, thus validating the sheep model for postmortem studies of the human brain (Fig. 22A). Another group studied pig brains using the same technique, and similar time courses for some analytes were described. The investigations on postmortem decomposition by H MRS may represent real progress in the field for the following reasons: a noninvasive in situ chemical analysis is possible with quantitation of analytes; longitudinal studies of postmortem changes with reproducible results are possible; the sheep model seems to be valid for studying human brains; influencing factors such as temperature can be easily

studied in this model; the definition of analytic functions for the time courses of 10 metabolites up to 400 hpm was successful; prediction of the PMI based on the combination of five metabolites correlates well with the true time since death up to 250 hpm; and these metabolic changes cover a PMI, whereas no other method allows quantitative calculation of time of death with any acceptable degree of certainty.

Finally, this study shows that old problems in forensic medicine, such as estimating the time of death, can benefit from recent developments in modern imaging systems. It must be considered, however, that the preliminary experiments used isolated heads of animals, which were prepared by closing the spinal canal with Plasticine (GP Flair PLC, Cheam, UK), fixing it in a plastic holder, and storing it in a plastic container or bag. Different results were obtained in a study that compared metabolic changes in an isolated whole head and the head of an intact animal [107, 108]. Gas bubbles that developed in the brain tissue after 6–7 days in the isolated animal head and after 4–5 days in the head of the whole animal complicated the selection of a voxel entirely within homogeneous brain tissue and impaired spectroscopic measurements at longer PMIs. Quite different results were revealed when investigating metabolic alterations in the brain of the whole animal. Spectra showed differences as early as 48 hpm, but differences were especially apparent after longer PMIs. Significant differences in metabolic alterations during postmortem decomposition of the brain were demonstrated between the animal model with isolated heads and the intact animal. Decomposition in the intact animal appeared faster and probably differently than in the isolated head because of bacterial invasion from the gastrointestinal tract; such bacteria can reach the brain within a few days in a cadaver. Therefore, longitudinal studies on intact animals at different ambient temperatures are necessary.

Gastric contents

Gastric contents alone allows only a rough estimation of the interval between the last meal and death. The state of digestion and the distribution of the last meal in the stomach and upper intestine have long been proposed as a method to estimate the time of death. For such estimation, the volume of the stomach contents compared with the volume of the last meal and transportation distance to the small intestine must be known. Even if the volume of the last meal is not known, the type of meal (i.e., breakfast, lunch, or dinner) may allow rough estimation of the time of day when death occurred. Gastric emptying has been studied and quantified during the last few decades using various methods, including radiology, intubation aspiration, radioisotopes, ultrasonography, absorption kinetics of orally administered solutes, and ferromagnetic traces [95, 96].

Liquids leave the stomach much faster than solids. Whereas gastric emptying of liquids follows an exponential function, solids show a linear emptying pattern. The following gastric emptying times are given in the literature: 1–3 h for a light small-volume meal, 3–5 h for a medium-sized meal, and 5–8 h for a large meal. It must be kept in mind, however, that different anatomic and functional disorders can cause either delayed or more rapid gastric emptying (Table 15). According to Horowitz and Pounder [96], only the solid compartment of a mixed solid and liquid meal should be considered, and the weight of the stomach contents should be compared with an estimated weight of the last meal, with reference made to the known

Table 15 Etiology of delayed and rapid gastric emptying

(a) Transient delayed gastric emptying
Postoperative illness
Acute viral gastroenteritis
Hyperglycemia
Drugs: morphine, anticholinergics, levodopa, beta-adrenergic agonists, nicotine
Stress: labyrinthine stimulation, cold, pain, pectin supplementation
(b) Chronic gastric stasis
Diabetes mellitus
Postsurgical truncal vagotomy with pyloroplasty and antrectomy
Gastroesophageal reflux
Anorexia nervosa
Progressive systemic sclerosis
Chronic idiopathic intestinal pseudo-obstruction
Amyloidosis
Myotonic dystrophy
Familial dysautonomia
Dermatomyositis
Tachygastria
Paraplegia
Idiopathic myocardial infarction
Acute abdomen
Laparotomy
Physiological: liquids, acid, lipids, left side position
(c) Rapid gastric emptying
After gastric surgery
Vagotomy
Antrectomy/subtotal gastrectomy
Zollinger–Ellison syndrome
Duodenal ulcer disease
Reserpine
Physiological: liquids, hunger

Modified according to Horowitz and Pounder [96] and Tröger et al. [100]

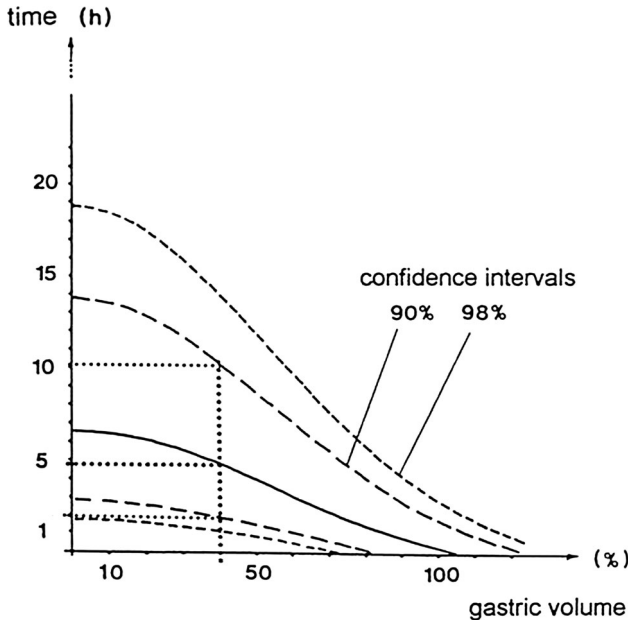

Fig. 23 Relationship between gastric volume of a mixed meal in % of ingested volume and time. With regression line and 90 and 98 % limits of confidence. From Tröger et al. [100]

50 % emptying times for the solid components of meals of various sizes.

Tröger et al. [100] compared the volume of the gastric contents found at autopsy with the time and volume of the last meals in an autopsy collection of 47 cases of sudden, unexpected death. Cases were excluded if there was a brain tumor, gastrointestinal tract surgery, intoxication, and/or alcoholism. Gastric content (% of the volume of the last meal) was plotted against the survival time. Only a gastric volume of >10 g was considered. The regression line and 90 and 98 % CIs were calculated (Fig. 23). The authors arrived at the following conclusions. If 50 % of the volume of the last meal was found at autopsy, the last food intake occurred about 3–4 h prior to death with a 98 % CI of 1–10 h. If 90 % of the last meal was found in the stomach, the last ingestion took place probably within the last hour prior to death with a 98 % CI of 3–4 h. However, conditions for delayed or rapid gastric emptying must be kept in mind (Table 15).

It is thus apparent that the factors affecting gastric emptying are multiple and complex. Attempting to use the state of digestion, rather than the quantity of food ingested, to determine the time of death is fraught with uncertainty [99].

Putrefaction

Putrefaction is a bacterial process predominantly influenced by environmental factors, mainly ambient temperature. Secondary factors include the presence of underlying disease and the body size. Advanced stages of putrefaction may be seen within a few hours after death, although in moderate or cold climates putrefaction may not appear for weeks. Even in relatively constant ambient temperatures, the progression of putrefaction varies considerably (Table 16). Recent H MRS investigations on metabolites emerging during decomposition of brain tissue have offered promising results, allowing even decomposition to be used as a reliable method of estimating the time of death. These longitudinal studies on postmortem changes, however, are still at an experimental level, and decomposition under various ambient temperatures must be studied. A weak point may be that decomposition has been studied in isolated brains and skulls, where invasion of bacteria from the gastrointestinal tract is not possible. There is no sound approach to using the stages of putrefaction, as shown in Table 16, to estimate the time of death while the body is lying in air. For bodies recovered from water, a reliable method for estimating the minimum and maximum time in water has been developed based on putrefactive changes that are visible during the external examination or dissection of the body. This is mainly because water temperature remains relatively constant over a long period of time and during day and night, whereas air temperature differs not only from day to night but also from one day to another.

Table 16 Progression of putrefaction of bodies in air temperatures of about 20 °C

After 1–2 days
Green discoloration of abdominal wall
Softening and decreased tension of eyeballs
After 3–5 days
Dark green discoloration of great parts of the abdominal wall
Some patchy green discoloration of the skin and other body regions
Body fluid leaking out from mouth and nostrils
After 8–12 days
Whole body surface dark green
Face, neck, and thoracic wall partly reddish-green
Bloating of abdomen, scrotum, face
Fingernails still fixed
Hair loose, begins to peel
After 14–20 days
Whole body green or reddish brown
Bloating of whole body
Blisters, partly filled with putrefactive fluid, partly burst with desiccation of the dermis
Eyes (iris, pupil, sclera) discolored reddish-brown
Fingernails peeling

According to Naeve [127]

Morphologic findings that are taken into consideration for estimating the duration of immersion are as follows.

External findings:

1. Rigor mortis
2. Lividity
3. Marbling
4. Bloating of raw face, scrotum, subcutaneous tissue
5. Discoloration of skin (green, black, reddish)
6. Loss of epidermis
7. Loss of hair
8. Hands and feet:

a) "Washerwoman's skin"
b) Loosening of nails
c) Peeling of skin
d) Loss of nails

Internal findings:

1. Volume of transudate in the pleural cavity
2. Heart without blood
3. Liquefaction of the brain

The warmer the water, the sooner a definitive stage of putrefaction occurs. The German forensic pathologist Reh [109, 110] developed a chart with the minimum time intervals of immersion based on the mean water temperature for each month and the stages of decomposition. Table 17 considers all 16 parameters for estimating the minimum time of immersion. On the left side are the useful criteria, followed by the months, the mean water temperature, and the minimum interval in days.

As many criteria as possible should be used to estimate the minimum interval since death. The result becomes more reliable when more than one or two criteria are used. The mean water temperature nearest to the actual water temperature at the time of recovery should be used to estimate the minimum time interval. Not only can the minimum time interval of immersion be estimated with this material, but the maximum interval can also be determined by considering criteria that have not yet developed. If during the month of June there is marbling, bloating, and discoloration of the body and the nails are loose but not lost, it may be concluded that the interval of immersion was >3 days but <8 days. Our personal experience with this chart is quite good; it is effective because it takes the actual temperature for the progression of putrefaction into consideration [111–115].

Immunohistochemical detection of insulin, thyroglobulin, and calcitonin

Although morphologic methods for estimating the time of death are of no practical value in forensic medicine, at least some studies on immunohistochemistry should be mentioned. Wehner et al. [116–120] studied whether the positive immunoreaction to various antigens such as insulin, thyroglobulin, or calcitonin is correlated with the time of death (Table 18). The theory behind these investigations is that with an increasing PMI, the tertiary structure of the antigen undergoes postmortem changes and becomes negative due to protein denaturation. Their results for thyroglobulin (Table 18) are as follows. The colloid and follicular cells of the thyroid glands showed a positive immunoreaction until 5 days postmortem, whereas these cells in none of the cadavers showed such a reaction beyond 13 days postmortem. Hence, a negative reaction indicates that the individual has been dead for >6 days, and a positive reaction indicates that the individual has been dead for <12 days. Pancreatic beta cells from ≤12-day-old cadavers produced a positive immunoreaction toward insulin in all cases, whereas no cells from >30-day-old cadavers showed such a reaction. These results indicate that in the case of a negative immunoreaction, the time of death can be assumed to be >12 days before the autopsy. When there is a positive stain, the death must have occurred ≤29 days earlier. Finally, in the above-mentioned studies, calcitonin was always detectable in thyroid C cells for up to 4 days. A negative staining result was always observed in >13-day-old bodies.

Immunohistochemical detection of antigens allows only a rough estimation of the time of death, which may be helpful in single cases. However, these time limits may change under different environmental conditions. Controlled studies on independent case material are still lacking. Our own preliminary results are promising [121]. Additionally, the data obtained by Wehner et al. [116–120] could be confirmed [121].

Conclusions

Several other methods for estimating the time of death using chemical methods should be addressed, including enzyme activity in various tissues and organs, morphologic changes, more VH and CSF analytes or other body tissues, protein degradation, and RNA or micro-RNA degradation [122–124]. Circadian patterns of gene expression have also been examined as a means of estimating the time of death (using circadian patterns as a biological clock) [125, 126]. All of these factors are of heuristic value for understanding decomposition, but they are not of practical relevance.

For practical purposes, there has been no real breakthrough in estimating the time of death by chemical methods. This is mainly because of the underlying processes (metabolic processes, autolysis, and putrefaction). Postmortem changes can be quantified, however, with such

Table 17 Estimation of minimum duration of immersion with various signs of putrefaction and maceration

Month	Jan	Feb	Mar	April	May	June	July	Aug	Sept	Oct	Nov	Dec
Median water temperature (°C)	3.5	3.9	5.8	9.9	13.0	17.4	18.6	18.6	17.3	13.2	8.8	4,7°
Marbling	32	25	16 (23)	9–10	4–5	2	1–2	2	3	4-5	10	17
Distension of tissues by gas	35	25	16 (23)	10	4–5	2–3	2	3	3–4	7	10	17
Discoloration of the body	35	25	16 (23)	(14)	4–5	2	2	3	3–4	7	10	17
Peeling of the epidermis	35	25	16 (23)	(16)	4–5	3	2	3	3–4	7	10	17
Hair loss	35	25	16 (23)	10–12	4–5	2–3	2–3	3	3–4	7	10	17
Hands: beginning of wrinkling	(1)	(1)	(12)			(6)			2		2	(1)
		28–30										
Hands: Nails become loose	>35	(40)	23	16	5	2-3	3	3	3-4	11	17	28
		30–32										
Hands: Peeling of skin in glove form	35	(45)	23	16	10	3	3	3-4	4	7	20	28
Hands: Nails lost	>53	45	30 (40)	21	14	8	3	4	10	>11	20	>35
Feet: Beginning of wrinkling	(1)	(1)	(12)	(1)		(6)	0.5		2		2	(1)
Feet: Nails become loose	>53	40	26 (35)	17	10	5	3	4	8	12	17	28
Feet: Peeling of skin	>53	60	35	16	10	5	3	5-6	8-9	>11 (14)	20	28
Feet: Nails lost	>53	>60	53	>35	>28	>10	3	>10	>10	>11	>20	>35
Transudate in pleural cavity*	35	25 (40)	18 (35)	10	5	3-4	3	3	11	5	>20	
Heart without blood	>39	32–34 (40)	23	14–15	9	4	3	3	5	11	20	28
Brain liquefied	35	30 (40)	(23)	14–16	5	3-4	3	3	6	10	17	28

Chart to estimate the minimum time interval of immersion. First line: month; second line: median water temperature for the month; left column: signs of putrefaction and maceration; following columns: minimal time interval in days. Example: If marbling, distension of tissues by gas, discoloration of the body, peeling of the epidermis, loosening of the fingernails and toenails, peeling of the skin of the hands and feet, and a liquefied brain are observed in July, the minimum time interval of immersion would be about 2–3 days

* >500 ml in adults

Table 18 Immunohistochemical detection of insulin, thyroglobulin, and calcitonin according to Wehner et al. [117–120]

	Positive staining	Negative staining
Insulin	≤12 days in all cases	>30 days in all cases
Thyroglobulin	≤5 days in all cases	>13 days in all cases
Calcitonin	≤4 days in all cases	>13 days in all cases

novel methods as flow cytometry, capillary zone electrophoresis, H MRS, and immunohistochemistry. Thus, extrapolation to the time of death is possible. It should be kept in mind, however, that the objective measurement of postmortem changes contributes in only small part to a more precise estimation of the time of death. Novel technology does not make the estimation by itself. Only when long-term longitudinal studies of the influencing factors (e.g., ambient temperature, local temperature at the site of measurement) that affect all postmortem changes are taken into account can the estimated time of death become more precise. Novel technology such as H MRS offers an excellent opportunity to study these factors.

It has become apparent that when examining the VH, we must avoid the analytic methods that have been validated for urine or serum. Methods optimized specifically for the VH must be developed for precise measurements.

Field studies are good indicators of practical value. To the best of our knowledge, however, field studies of chemical methods for estimating the time of death are almost completely missing in the literature compared, for instance, with studies of body cooling or supravital reactions. Thus, chemical methods appear to still be of academic interest only. Their importance may change in the future, when all of the previously mentioned criteria are fulfilled: quantitative measurement, mathematical descriptions, taking into account influencing factors quantitatively, declaration of precision, and proof of precision on independent material.

Many good scientific papers with ingenious formulas for estimating the time of death have been written. The aim of estimating the time of death is, according to Camps [94], to provide true scientific evidence and avoid miscarriage of justice at all cost.

Sixty years ago, Camps [94] stated that in some people's minds, the time of death somewhat resembles the value attributed to a lie detector. Estimating the time of death at the scene of a crime is often not an exact science. The best we can achieve is a reasoned guess by taking into account all known

Table 19 Design of studies on postmortem changes

Underlying process (physical, metabolic, physicochemical, bacterial, autolysis and diffusion, entomology, radiocarbon dating)
Clear definition of site of measurement or site of sample acquisition
Longitudinal studies with objective measurement of postmortem changes
Quantitative consideration of influencing factors such as ambient temperature or temperature at the site of measurement
Consideration of interindividual variability
At different times postmortem (10, 20, 30…hpm) (time dependence), investigations on postmortem changes/taking samples should be carried out; however, investigations should involve varying ambient temperatures (differing ambient temperatures for same postmortem interval). This time-saving procedure allows a first estimation of the variability in comparison with the standard methods
Validation of method
Calculation of data on precision, accuracy, and reliability
Control studies on independent case material to check the accuracy of the method
Field studies on cases with known time since death to check the practical applicability, reliability, and accuracy
Comparison with standard methods to check for improvement
Determination of whether the method can be used together with the standard methods
When methods are compared, they must have the same postmortem interval
Case material should comprise different causes of death (diseases and duration of terminal episodes may be vital points for the strength of the correlation between investigated parameters and the postmortem interval)

factors. Our aim should be to limit the margin of error inherent in assessing the effects of these factors.

Progress in the field of death time estimation usually requires long-term research and a strict study design (Table 19). Research must focus for years on a special problem arising from the basic idea to validate the method over field studies to prove the accuracy and reliability of the method.

Key Points

1. The main principle of determining the time since death is calculation of measurable data along a time-dependent curve back to the starting point.
2. Medicolegal death time estimation must estimate the time since death reliably; reliability is the most important principle and can only be derived empirically by statistical analysis of errors in field studies.
3. The different methods used to estimate time since death vary greatly in nature.
4. The gold standard for estimating the time since death in forensic practice in the early postmortem interval is the nomogram method based on the two-exponential formula of body cooling developed by Marshall and Hoare [26].
5. Several methods, such as assessment of supravital reactions, rigor mortis, and postmortem lividity (the compound method), are used to increase the precision of death time estimation. Chemical methods of estimating the time since death may be of importance in the future if influencing factors such as preexisting diseases and ambient temperature (i.e., vitreous potassium concentration) are taken into account or new technologies (H magnetic resonance spectroscopy) are used to study putrefactive changes.

References

1. Henssge C, Madea B. Methoden zur Bestimmung der Todeszeit an Leichen. Lübeck: Schmidt-Römhild-Verlag; 1988.
2. Henssge C, Madea B. Estimation of the time since death in the early post-mortem period. Forensic Sci Int. 2004;144:167–75.
3. Henssge C, Madea B. Estimation of time since death. Forensic Sci Int. 2007;165:182–4.
4. Madea B. Handbook of forensic medicine. Chichester: Wiley; 2014.
5. Madea B, Henssge C. Timing of death. In: Payne-James J, Busuttil A, editors. Forensic Medicine: clinical and pathological aspects. London: Greenwich Medical Media Limited; 2003. p. 91–114.
6. Madea B. Rechtsmedizin: Befunderhebung, Rekonstruktion, Begutachtung. 3rd ed. Berlin: Springer; 2015.
7. Albrecht A, Gerling I, Henssge C. Zur Anwendung des Rektaltemperatur-Todeszeit-Nomogramms am Leichenfundort. Z Rechtsmed. 1990;103:257–78.
8. Althaus L, Henssge C. Rectal temperature time of death nomogram: sudden change of ambient temperature. Forensic Sci Int. 1999;99:171–8.
9. Brown A, Marshall TK. Body temperature as a means of estimating the time of death. Forensic Sci. 1974;4:125–33.
10. De Saram GSW, Webster G, Kathirgamatamby N. Post-mortem temperature and the time of death. J Crim Law Criminol. 1955;46:562–77.
11. Henssge C. Rectal temperature time of death nomogram: dependence of corrective factors on the body weight under stronger thermic insulation conditions. Forensic Sci Int. 1992;54:51–6.
12. Henssge C. Precision of estimating the time of death by mathematical expression of rectal body cooling. Z Rechtsmed. 1979;83:49–67.

13. Henssge C. Death time estimation in case work I. The rectal temperature time of death nomogram. Forensic Sci Int. 1988;38:209–36.
14. Henssge C. Temperature based methods II. In: Henssge C, Knight B, Krompecher T, Madea B, Nokes L, editors. The estimation of the time since death in the early post-mortem period. 2nd ed. London: Edward Arnold; 2002.
15. Henssge C, Beckmann ER, Wischhusen F, Brinkmann B. A Determination of time of death by measuring central brain temperature. Z Rechtsmed. 1984;93:1–22.
16. Henssge C, Frekers R, Reinhardt S, Beckmann ER. Determination of time of death on the basis of simultaneous measurement of brain and rectal temperature. Z Rechtsmed. 1984;93:123–33.
17. Henssge C, Hahn S, Madea B. Praktische Erfahrungen mit einem Abkühlungsdummy. Beitr Gerichtl Med XLIV. 1986;123–126.
18. Henssge C, Madea B, Schaar U, Pitzken C. Die Abkühlung eines Dummy unter verschiedenen Bedingungen im Vergleich zur Leichenabkühlung. Beitr Gerichtl Med XLV. 1987;145–149.
19. Henssge C, Madea B, Gallenkemper E. Death time estimation in case work II. Integration of different methods. Forensic Sci Int. 1988;39:77–87.
20. Henssge C, Althaus L, Bolt J, Freislederer A, Haffner HT, Henssge CA, et al. Experiences with a compound method for estimating the time since death. I. Rectal temperature nomogram for time since death. II. Integration of non-temperature-based methods. Int J Legal Med. 2000;6:303–31.
21. Henssge C, Madea B. Frühe Leichenerscheinungen und Todeszeitbestimmung im frühpostmortalen Intervall. In: Brinkmann B, Madea B, editors. Handbuch Rechtsmedizin, vol. I. Berlin: Springer; 2004.
22. Henssge C. Basics and application of the 'nomogram method' at the scene. In: Madea B, editor. Estimation of the time since death. 3rd ed. Boca Raton: Taylor & Francis Group/CRC Press; 2015. p. 63–114.
23. Henssge C, Madea B. Practical casework. Integration of different methods in casework. In: Madea B, editor. Estimation of the time since death. 3rd ed. Boca Raton: CRC Press; 2015. p. 227–37.
24. Hubig M, Muggenthaler H, Mall G. Finite element method in temperature-based death time determination. In: Madea B, editor. Estimation of the time since death. 3rd ed. Boca Raton: CRC Press; 2015. p. 114–33.
25. Hubig M, Muggenthaler H, Sinicina I, Mall G. Temperature based forensic death time estimation: The standard model in experimental test. Legal Medicine. Tokyo; 2015.
26. Marshall TK, Hoare FE. I Estimating the time of death. The rectal cooling after death and its mathematical expression. II The use of the cooling formula in the study of postmortem body cooling. III The use of the body temperature in estimating the time of death. J Forensic Sci. 1962;7:56–81, 189–210, 211–221.
27. Hunnius PV, Mallach HJ, Mittmeyer HJ. Quantitative pressure measurements of livores mortis relative to the determination of the time of death. Z Rechtsmed. 1973;73:325–44.
28. Madea B, Knight B. Postmortem lividity. In: Madea B, editor. Estimation of the time since death. 3rd ed. Boca Raton: CRC Press; 2015. p. 59–62.
29. Mallach HJ. Zur Frage der Todeszeitbestimmung. Berl Med. 1964;18:577–82.
30. Mallach HJ, Mittmeyer HJ. Totenstarre und Totenflecke. Z Rechtsmed. 1971;69:70–8.
31. Rosendahl W, Döppes D. Radiocarbon dating. Basic principles and applications. In: Madea B, editor. Estimation of the time since death. 3rd ed. Boca Raton: CRC Press; 2015. p. 259–67.
32. Bate-Smith EC, Bendall JR. Rigor mortis and adenosinetriphosphate. J Physiol. 1947;106:177–85.
33. Bate-Smith EC, Bendall JR. Factors determining the time course of rigor mortis. J Physiol. 1949;110:47–65.
34. Beier G, Liebhardt E, Schuck M, Spann M. Measurement of rigor mortis on human skeletal muscles in situ. Z Rechtsmed. 1977;79:277–83.
35. Krompecher T, Bergerioux C. Experimental evaluation of rigor mortis. VII. Effect of ante- and postmortem electrocution on the evolution of rigor mortis. Forensic Sci Int. 1988;38:27–35.
36. Krompecher T, Fryc O. Experimentelle Untersuchungen an der Leichenstarre unter Einfluss von körperlicher Anstrengung. Beitr Gerichtl Med. 1978;36:345–9.
37. Krompecher T, Fryc O. Experimental evaluation of rigor mortis. III. Comparative study of the evolution of rigor mortis in different sized muscle groups in rats. Forensic Sci Int. 1978;12:97–102.
38. Krompecher T, Fryc O. Experimental evaluation of rigor mortis. IV. Change in strength and evolution of rigor mortis in the case of physical exercise preceding death. Forensic Sci Int. 1978;12:103–7.
39. Krompecher T, Fryc O. Zur Frage der Todeszeitbestimmung auf Grund der Leichenstarre. Beitr Gerichtl Med. 1979;37:285–9.
40. Krompecher T, Fryc O. Experimental evaluation of rigor mortis. V. Effects of temperature on the evolution of rigor mortis. Forensic Sci Int. 1981;17:19–26.
41. Krompecher T. Rigor mortis: estimation of the time since death by the evaluation of the cadaveric rigidity. In: Henssge C, Knight B, Krompecher T, Madea B, Nokes L, editors. The estimation of the time since death in the early postmortem period. 2nd ed. London: Edward Arnold; 2002. p. 144–60.
42. Krompecher T. Rigor Mortis. In: Madea B, editor. Estimation of the time since death. 3rd ed. Boca Raton: CRC Press; 2015. p. 41–57.
43. Madea B, Krompecher T, Knight B. Muscles and tissue changes after death. In: Henssge C, Knight B, Krompecher T, Madea B, Nokes L, editors. The estimation of the time since death in the early postmortem period. 2nd ed. London: Edward Arnold; 2002.
44. Dotzauer G. Idiomuskulärer Wulst und postmortale Blutung. Dtsch Z Gerichtl Med. 1958;46:761–71.
45. Madea B. Längsschnittuntersuchungen zur supravitalen elektrischen Erregbarkeit der Skelettmuskulatur. I. Objektivierung der supravitalen Muskelkontraktion. Rechtsmed. 1990;2:107–21.
46. Madea B. Längsschnittuntersuchungen zur supravitalen elektrischen Erregbarkeit der Skelettmuskulatur. II. Quantifizierung der supravitalen Muskelkontraktion. Rechtsmed. 1990;3:44–50.
47. Madea B. Estimating time of death from measurement of electrical excitability of skeletal muscle. J Forensic Sci Soc. 1992;32:117–29.
48. Madea B, Henssge C. Electrical excitability of skeletal muscle postmortem in casework. Forensic Sci Int. 1990;47:207–27.
49. Madea B, Rödig A. Precision of estimating the time since death using different criteria of excitability. For Sci Med Pathol. 2006;2:127–33.
50. Madea B. Supravitality in tissues. In: Madea B, editor. Estimation of the time since death. 3rd ed. Boca Raton: CRC Press; 2015. p. 17–40.
51. Berg S. Todeszeitbestimmung in der spätpostmortalen Phase. In: Brinkmann B, Madea B, editors. Handbuch Gerichtliche Medizin, vol. 1. Berlin: Springer; 2004. p. 191–204.
52. Bonte W. Der postmortale Proteinkatabolismus. Experimentelle Untersuchungen zum Problem der forensischen Leichenzeitbestimmung. Habilitationsschrift, Göttingen: Medizinische Fakultät der Georg-August-Universität Göttingen; 1978.

53. Madea B. Is there recent progress in the estimation of the postmortem interval by means of thanatochemistry? Forensic Sci Int. 2005;151:139–49.
54. Madea B, Preuss J, Musshoff F. From flourishing life to dust—the natural cycle of growth and decay. In: Wieczorek A, Rosendahl W, editors. Mummies of the world. Munich: Prestel; 2010. p. 14–29.
55. Madea B, Kernbach-Wighton G. Autolysis (self-digestion). In: Madea B, editor. Estimation of the time since death. 3rd ed. Boca Raton: CRC Press; 2001. p. 153–61.
56. Rutty G, Morgan B. Cross-sectional imaging and the postmortem interval. In: Madea B, editor. Estimation of the time since death. 3rd ed. Boca Raton: CRC Press; 2015. p. 269–75.
57. Adelson L, Sunshine I, Rushforth NB, Mankoff M. Vitreous potassium concentration as an indicator of the postmortem interval. J Forensic Sci. 1963;8:503–14.
58. Adjudantis G, Coutselinis A. Estimation of the time of death by potassioum levels in the vitreous humour. Forensic Sci. 1972;1:55–60.
59. Bortolotti F, Pascali JP, Davis GG, Smith FP, Brissie RM, Tagliaro F. Study of vitreous potassium correlation with time since death in the postmortem range from 2 to 110 hours using capillary ion analysis. Med Sci Law. 2011;51(Suppl 1):S20–3.
60. Coe JI. Vitreous potassium as a measure of the postmortem interval: an historical review and critical evaluation. Forensic Sci Int. 1989;42:201–13.
61. Coe JI. Postmortem chemistry update. Emphasis on forensic application. Am J Forensic Med Pathol. 1993;14:91–117.
62. Hansson L, Uotila U, Lindfors R, Laiho K. Potassium content of the vitreous body as an aid in determining the time of death. J Forensic Sci. 1966;11:390–4.
63. James RA, Hoadley PA, Sampson BG. Determination of postmortem interval by sampling vitreous humour. Am J Forensic Med Pathol. 1997;18:158–62.
64. Jashnani KD, Kale SA, Rupani AB. Vitreous humor: biochemical constituents in estimation of postmortem interval. J Forensic Sci. 2010;55:1523–7.
65. Klein A, Klein S. Todeszeitbestimmung am menschlichen Auge. MD Thesis, Dresden University; 1978.
66. Lange N, Swearer S, Sturner WQ. Human postmortem interval estimation from vitreous potassium: an analysis of original data from six different studies. Forensic Sci Int. 1994;66:159–74.
67. Madea B, Henssge C, Hönig W, Gerbracht A. References for determining the time of death by potassium in the vitreous humour. Forensic Sci Int. 1989;8:231–43.
68. Madea B, Herrmann N, Henssge C. Precision of estimating the time since death by vitreous potassium—comparison of two different equations. Forensic Sci Int. 1990;46:277–84.
69. Madea B, Käferstein H, Herrmann N, Sticht G. Hypoxanthine in vitreous humour and cerebrospinal fluid—a marker of postmortem interval and prolonged (vital) hypoxia? Remarks also on hypoxanthine in SIDS. Forensic Sci Int. 1994;65:19–31.
70. Madea B, Kreuser C, Banaschak S. Postmortem biochemical examination of synovial fluid—a preliminary study. Forensic Sci Int. 2001;118:29–35.
71. Madea B, Henssge C. Eye changes after death. In: Henssge C, Knight B, Krompecher T, Madea B, Nokes L, editors. The estimation of the time since death in the early postmortem period. 2nd ed. London: Edward Arnold; 2002.
72. Madea B, Rödig A. Time of death dependent criteria in vitreous humor—precision of estimating the time since death. Forensic Sci Int. 2006;164:87–92.
73. Madea B, Henssge C. Eye changes after death. In: Madea B, editor. Estimation of the time since death. 3rd ed. Boca Raton: CRC Press; 2015. p. 161–85.
74. Madea B, Henssge C. Cerebrospinal fluid chemistry. In: Madea B, editor. Estimation of the time since death. 3rd ed. Boca Raton: CRC Press; 2015. p. 186–9.
75. Mathur A, Agrawal YK. An overview of methods used for estimation of time since death. Aust J Forensic Sci. 2011;43:275–85.
76. Mihailovic Z, Atanasijevic T, Popovic V, Milosevic MB, Sperhake JP. Estimation of the postmortem interval by analyzing potassium in the vitreous humor: could repetitive sampling enhance accuracy? Am J Forensic Med Pathol. 2012;33:400–3.
77. Munoz JI, Suarez-Penaranda JM, Otero XL, Rodriguez-Calvo MS, Costas E, Miguens X, et al. A new perspecitive in the estimation of postmortem interval (PMI) based on vitreous. J Forensic Sci. 2001;45:209–2014.
78. Munoz Barus JI, Suarez-Penaranda J, Otero XL, Rodriguez-Calvo MS, Costas E, Miguens X, et al. Improved estimation of postmortem interval based on differential behavior of vitreous potassium and hypoxanthine in death by hanging. For Sci Int. 2002;125:67–74.
79. Pounder J. Postmortem interval. In: Siegel JA, Saukko PJ, Knupfer GC, editors. Encyclopaedia of forensic sciences, vol. 3. San Diego: Academic Press; 2000. p. 1167–72.
80. Rognum TO, Hauge S, Oyasaeter S, Saugstad OD. A new biochemical method for estimation of postmortem time. For Sci Int. 1991;51:139–46.
81. Siddamsetty AK, Verma SK, Kohli A, Puri D, Singh A. Estimation of time since death form electrolyte, glucose and calcium analysis of postmortem vitreous humour in semi-arid climate. Med Sci Law. 2014;54:158–66.
82. Stephens RJ, Richards RG. Vitreous humor chemistry: the use of potassium concentration for the prediction of the postmortem interval. J Forensic Sci. 1987;32:503–9.
83. Sturner WQ. The vitreous humour: postmortem potassium changes. Lancet. 1963;1:807–8.
84. Sturner WQ, Gantner GE. The postmortem interval. A study of potassium in the vitreous humor. Am J Clin Pathol. 1964;42:137–44.
85. Tumrana NK, Ambadea VN, Dongreb AP. Thanatochemistry: study of vitreous humor potassium. Alexandria J Med. 2014;50:365–8.
86. Zhou B, Zhang L, Zhang G, Zhang X, Jiang X. The determination of potassium concentration in vitreous humor by low pressure ion chromatography and its application in the estimation of postmortem interval. J Chromatogr B Analyt Technol Biomed Life Sci. 2007;852:278–81.
87. Zilg B, Bernard S, Alkass K, Berg S, Druid H. A new model for the estimation of time of death from vitreous potassium levels corrected for age and temperature. For Sci Int. 2015;254:158–66.
88. Zilg B. Postmortem analyses of virtreous fluid. MD Thesis, Department of Oncology-Pathology. Karolinska Institutet, Stockholm, Sweden; 2015.
89. Reibe S, Doetinchem PV, Madea B. A new simulation-based model for calculating post-mortem intervals using developmental data for Lucilia sericata (Dipt.: Calliphhoridae). Parasitol Res. 2010;107:9–16.
90. Reibe S, Madea B. How promptly do blowflieds colonise fresh carcasses? A study comparing indoor with outdoor locations. For Sci Int. 2010;195:52–7.
91. Reibe S, Madea B. Use of Megaselia scalaris (Dipt.: Phoridae) for post-mortem interval estimation indoors. Parasitol Res. 2010;106:637–40.
92. Reibe S. Forensic entomolgy. In: Madea B, editor. Estimation of the time since death. 3rd ed. Boca Raton: CRC Press; 2015. p. 249–57.

93. Van den Oever R. A review of the literature as to the present possibilities and limitations in estimating the time of death. Med Sci Law. 1976;16:269–76.
94. Camps FE. Establishment of the time of death—a critical assessment. J Forensic Sci. 1959;4:73–82.
95. Horowitz M, Maddern GJ, Chatterton BE, Collins PJ, Harding PE, Sherman DJC. Changes in gastric emptying rates with age. Clin Sci. 1984;67:213–8.
96. Horowitz M, Pounder DJ. Gastric emptying—forensic implications of current concepts. Med Sci Law. 1985;25:201–14.
97. Madea B, Henssge C. Historisches zur Todeszeitbestimmung. Z Rechtsmed. 1985;95:19–25.
98. Madea B, Oehmichen M, Henssge C. Postmortaler Transport von Mageninhalt. Z Rechtsmed. 1986;97:201–6.
99. Madea B, Knight B. Gastric contents and time since death. In: Madea B, editor. Estimation of the time since death. 3rd ed. Boca Raton: CRC Press; 2015. p. 213–22.
100. Tröger HD, Baur C, Spann KW. Mageninhalt und Todeszeitbestimmung. Lübeck: Schmidt-Römhild; 1987.
101. Madea B, Henssge C. General remarks on estimating the time since death. In: Madea B, editor. Estimation of the time since death. 3rd ed. Boca Raton: CRC Press; 2015. p. 1–6.
102. Knight B, Madea B. Historical review on early work on estimating the time since death. In: Madea B, editor. Estimation of the time since death. 3rd ed. Boca Raton: CRC Press; 2015. p. 7–16.
103. Madea B. Importance of supravitality in forensic medicine. Forensic Sci Int. 1994;69:221–41.
104. Rutty G. The use of temperatures recorded from the external auditory canal for the estimation of the postmortem interval. In: Madea B, editor. Estimation of the time since death. 3rd ed. Boca Raton: CRC Press; 2015. p. 134–51.
105. Biermann FM, Potente S. The deployment of conditional probability distributions for death time estimation. Forensic Sci Int. 2011;210:82–6.
106. Potente S. Practical casework. Conditional probability in death time estimation. In: Madea B, editor. Estimation of the time since death. 3rd ed. Boca Raton: CRC Press; 2015. p. 237–48.
107. Musshoff F, Klotzbach H, Block W, Traeber F, Schild H, Madea B. Comparison of post-mortem metabolic changes in sheep brain tissue in isolated heads and whole animals using 1H-MR spectroscopy—preliminary results. Int J Legal Med. 2011;125:741–4.
108. Musshoff F, Madea B. H^3-Magnetic resonance spectroscopy. In: Madea B, editor. Estimation of the time since death. 3rd ed. Boca Raton: CRC Press; 2015. p. 203–12.
109. Reh H. Diagnostik des Ertrinkungstodes und Bestimmung der Wasserzeit. Düsseldorf: Triltsch; 1969.
110. Reh H. Anhaltspunkte für die Bestimmung der Wasserliegezeit. Dtsch Z Ges Gerichtl Med. 1967;59:235–45.
111. Doberentz E, Madea B. Schätzung der Wasserliegezeit. Retrospektive Untersuchung zur Reliabilität. Rechtsmed. 2010;20:393–9.
112. Doberentz E, Madea B. Estimating the time of immersion of bodies found in water—an evaluation of a common method to estimate the minimum time interval of immersion. Revista Espanola de Medicina Legal. 2010;36:51–61.
113. Doberentz E, Madea B. Estimation of duration of immersion. In: Madea B, editor. Estimation of the time since death. 3rd ed. Boca Raton: CRC Press; 2015. p. 189–202.
114. Madea B. Estimation of duration of immersion. Nordisk Rettsmedisin. 2002;8:4–10.
115. Madea B, Stockhausen S, Doberentz E. Bestimmung der Wasserliegezeit nach Reh – weitere Untersuchungen zur Prüfung der Reliabilität. Arch Kriminol. 2016;237:1–2.
116. Wehner F. Die Eingrenzung der Leichenliegezeit im spätpostmortalen Intervall. Neue Ansätze mittels immunhistochemischer. Verfahren Med Welt. 2009;11–12:402–6.
117. Wehner F, et al. Delimitation of the time of death by immunohistochemical insulin detection in pancreatic ß-cells. Forensic Sci Int. 1999;105:161–9.
118. Wehner F, et al. Delimitation of the time of death by immunohistochemical detection of thyroglobulin. Forensic Sci Int. 2000;110:199–206.
119. Wehner F, Wehner H-D, Subke J. Delimitation of the time of death by immunohistochemical detection of calcitonin. Forensic Sci Int. 2001;122:89–94.
120. Wehner F, Wehner H-D, Subke J. Delimitation of the time of death by immunohistochemical detection of glucagon on pancreatic ß-cells. Forensic Sci Int. 2002;124:241–8.
121. Madea B. Immunohistochemical methods as an aid in estimating the time since death. In: Madea B, editor. Estimation of the time since death. 3rd ed. Boca Raton: CRC Press; 2015. p. 223–5.
122. Ondrizola A, Riancho JA, de la Vega R, Agudo G, Garcia-Blanco A, de Cos E, et al. miRNA analysis in vitreous humor to determine the time of death: a proof-of-concept pilot study. Int J Legal Med. 2013;127:573–8.
123. Zubakov D, Kokshoorn M, Kloosterman A, Kayser M. New markers for old stains: stable mRNA markers for blood and saliva identification from up to 16-years-old stains. Int J Legal Med. 2009;123:71–4.
124. Sampaio-Silva F, Magalhaes T, Carvalho F, Dinis-Oliveira RJ, Silvestre R. Profilingo f RNA degradation for estimation of post mortem interval. PLoS ONE. 2013;8:e56507.
125. Li JZ, Bunney BG, Meng F, Hagenauer MH, Walsh DM, Vawter MP, et al. Circadian patterns of gene expression in the human brain and disruption in major depressive disorder. PNAS. 2013;110:9950–5.
126. Kimura A, Ishida Y, Hayashi T, Nosaka M, Kondo T. Estimating time of death based on the biological clock. Int J Legal Med. 2011;125:385–91.
127. Naeve W. Gerichtliche Medizin für Polizeibeamte. Heidelberg: Kriminalistik Verlag; 1978.